BLOCK COPOLYMER INTEGRAL ASYMMETRIC MEMBRANES USING SNIPS PROCESS

A Thesis

Presented to the Faculty of the Graduate School

of Cornell University

In Partial Fulfillment of the Requirements for the Degree of

Master of Science

by

Parth Nitin Vaidya

August 2017

ABSTRACT

Over the last decade, membranes prepared using block copolymer self-assembly and non-solvent induced phase separation (SNIPS) process have become increasingly desirable candidates for water purification and protein separation applications due to their excellent permselectivity. However, biofouling is a major problem encountered in the filtration process as it may lead to a reduction in effective pore size, pore blockage and formation of a biofilm on the membrane surface. Thus, there is a pressing need to design new systems that incorporate an anti-fouling property while retaining the high performance capabilities of SNIPS membranes. Poly(ethylene oxide) (PEO) is a promising candidate to reduce membrane fouling due to its hydrophilic nature. To date it has remained challenging to extend the SNIPS process to new polymers with PEO end block, including poly(isoprene-*b*-styrene-*b*-ethylene oxide) (ISO), which involves optimizing a multitude of parameters to obtain desired membrane structure and performance.

To overcome this impediment, two chemically distinct triblock terpolymers, poly(isoprene-*b*-styrene-*b*-(4-vinyl) pyridine) (ISV) and ISO were blended in the dope solution in order to fabricate membranes using the SNIPS process. The weight ratio of ISV to ISO in the blended solutions was varied. Scanning Electron Microscopy (SEM) images of both the pure ISV and blended membranes reveal a mesoporous skin layer atop a macroporous substructure. The asymmetric membranes from 9:1 and 7:3 blends retained their pH-responsive permeability behavior characteristic to pure ISV

membranes. Additionally, about a three-fold decrease in protein adsorption was observed in 5:5 blended membranes compared to pure ISV, likely due to the antifouling property of PEO. Thus, the blended membranes exhibit properties characteristic of the chemistries present in both the parent block copolymers. This study corroborates the ability and ease of the SNIPS process combined with a facile "mix and match" approach to access and tailor unique chemical functionalities in a single membrane opening doors to previously challenging property combinations.

BIOGRAPHICAL SKETCH

Parth Vaidya was born and brought up in Thane, India, to Nitin and Shubhada Vaidya. Parth attended elementary, middle and high school at Smt. Sulochanadevi Singhania School, Thane, from 1999 through 2011. During this time, he was an active member of the school honor society for academic excellence. He also actively took part in extra-curricular activities such as national science olympiads, and various sports such as badminton and swimming.

Parth joined the Institute of Chemical Technology in Mumbai, India to pursue his undergraduate studies in Oils, Oleochemicals and Surfactants Technology. Through some courses taken during the sophomore year of college, he discovered his keen interest in polymeric materials. He started researching on bio-based poly(ester amide) hot melt adhesives under the supervision of Prof. S.T. Mhaske, and was able to co-author several papers based on his work. His undergraduate research work further strengthened his interest in pursuing Materials Science for graduate studies.

For his Master's studies at Cornell University, Parth moved to Ithaca, NY, in the Fall of 2015. He worked in Prof. Ulrich Wiesner's group on block copolymer based asymmetric membranes fabricated using the SNIPS process. The work described in the thesis summarizes results obtained during his research in the Wiesner group.

DEDICATED TO MY FAMILY AND FRIENDS

ACKNOWLEDGMENTS

There are many individuals that I would like to thank, for both active and indirect help and support in completion of this thesis. Firstly, I would like to thank my thesis advisor Prof. Ulrich Wiesner for giving me this opportunity to work on the challenging and interesting SNIPS membrane project. His scientific acumen and motivation has been critical in completion of this work. I would also like to thank my special committee member Prof. Yong Joo for his support.

I would like to thank the Wiesner group members for their unending help and support. In particular, I am indebted to Yuk Mun Li who mentored me during my research, right from making my first polymer to conducting performance measurements on the SNIPS membranes. Additionally, I would like to particular thank Qi Zhang and Fumiaki Matsuoka for their help in synthesizing my ISO terpolymer and fruitful discussions that greatly helped in my work. I am also grateful to Peter Beaucage and Dr. Kate Barteau for conducting SAXS measurements on my samples at CHESS and for their technical insights. I would also like to express my gratitude to Swathi Rao, Sarah Hesse, Kasia Oleske, Zihao Zhang and R. Paxton Thedford for helpful discussions and motivating me during this work. I would also like to thank Michele Conrad and Kyle Page for their administrative help. For helping me with training on the Mira and Keck SEM, I would like to thank Don Werder and Mick Thomas (CCMR).

Finally, I am forever grateful to my parents, family and friends, for their tireless love, support and belief in me.

TABLE OF CONTENTS

LIST OF FIGURES

LIST OF TABLES

LIST OF ABBREVIATIONS

FFT – Fast Fourier Transform

GISAXS – Grazing incidence small-angle X-ray scattering

GPC – Gel Permeation Chromatography

ISO – Poly(isoprene-*b*-styrene-*b*-ethylene oxide)

ISV – Poly(isoprene-*b*-styrene-*b*-(4-vinyl)pyridine)

NIPS – Non-solvent induced phase separation

NMR – Nuclear magnetic resonance

P4VP- Poly(4-vinylpyridine)

PDI – Polydispersity index

PEO – Poly(ethylene oxide)

SAXS – Small-angle X-ray Scattering

SEM – Scanning electron microscopy

SNIPS – Self-assembly and non-solvent induced phase separation

CHAPTER 1

INTRODUCTION

1.1 Abstract

The work described in this thesis involves the fabrication, characterization and performance measurements of block copolymer membranes prepared using the self-assembly and non-solvent induced phase separation (SNIPS) process. In a first part, an ineffective attempt is described to employ poly(isoprene-*b*-styrene-*b*-ethylene oxide) (ISO) triblock terpolymer in the fabrication of antifouling membranes. To overcome this hurdle, two chemically distinct triblock terpolymers, poly(isoprene-*b*-styrene-*b*-(4-vinyl)pyridine) (ISV) and ISO are subsequently blended in the dope solution in order to fabricate pH-responsive and antifouling membranes using the SNIPS process. This chapter briefly introduces basic concepts of polymers, anionic polymerization procedure and block copolymer self-assembly. Furthermore, the phase inversion approach to asymmetric ultrafiltration (UF) membranes is introduced together with its combination with block copolymer self-assembly resulting in what is now called the SNIPS method for UF membrane fabrication.

1.2 Polymers

Polymers are formed by linking together repeating units of a number of small molecules called monomers. A wide variety of polymers, also called macromolecules, are found naturally or can be synthetically prepared in the laboratory. For example, DNA and proteins are polymers extensively found in nature while synthetic plastics such as polystyrene are widely used in our daily lives.

Polymers can be classified in numerous ways. Based on their skeletal structure, polymers can be classified as linear or non-linear. Linear polymers have only two defined chain ends. Non-linear polymers such as branched polymers have a number of side-chains attached to the main backbone chain. Other non-linear polymers exist, such as network polymers and cross-linked polymers. Depending on the monomeric unit that they are comprised of, polymers can be classified as either homopolymers or copolymers. Homopolymers and copolymers are polymers derived from a single monomeric species or from multiple monomeric species, respectively. Copolymers are further divided into various sub-categories such as statistical copolymers, alternating copolymers, block copolymers and graft copolymers. The most common method of classifying polymers in industry is into thermoplastics, elastomers and thermosetting plastics. Thermoplastics are linear or branched polymers that can be melt processed on application of heat into molds of various shapes that are retained on cooling to room temperature into the solid. Elastomers are crosslinked rubbery polymers that can be stretched easily by applying stress and can rapidly recover their original dimensions on removal of the applied stress. Thermosetting plastics or thermosets are generally rigid materials and unlike thermoplastics, they degrade rather than melt on application

of heat.[1]

Polymers are characterized by the total number of repeating units of monomers per chain of the polymer, called the degree of polymerization. Generally, synthetic polymers consist of macromolecular chains with a distribution of molar masses. The most widely used way of expressing polymer molar mass is by either the number average molar mass, M_n, or the weight average molar mass, M_w, defined in equations 1.2.1 and 1.2.2.[2]

$$Mn = \frac{\sum M_i N_i}{\sum N_i} \tag{1.2.1}$$

$$Mw = \frac{\sum M_i^2 N_i}{\sum M_i N_i} \tag{1.2.2}$$

$$PDI = M_w \,/\, M_n \tag{1.2.3}$$

For a polydisperse polymer, the value of the polydispersity index, *PDI*, as described in equation (1.2.3) must be by definition greater than unity. Depending on the polymerization technique, PDI's range from values close to 1 for living polymerizations to 10 for uncontrolled radical polymerizations. The closer this value is to 1.0, the narrower is the weight distribution of the polymer and the less polydisperse it is.

The process to chemically link monomers to form a polymer is called as polymerization. Depending on the underlying mechanism of polymerization, polymers

can be prepared either by *step-growth* polymerization or by *chain-growth* polymerization.[2] In step-growth polymerizations any two species within the reactor can react with one another. At low conversions there is a very slow molar mass growth rate. Only at very high conversions (>95%) do polymers formed by step-growth polymerization reach moderately high molar mass. Representative reactions belonging to this class of polymerization are *polyaddition* and *polycondensation* reactions.[1,3]

In chain-growth polymerizations the polymer grows by addition of one monomer after the other with the reactive end-group of a growing polymeric chain. The reaction in this type of polymerization can be divided into three distinct stages: *initiation*, *propagation* and *termination*. Representative reactions belonging to this class of polymerization are *free-radical polymerization* and *ionic polymerization*. Free-radical polymerization is the most widely used method of chain-growth polymerization to produce polymers such as poly(ethylene), poly(styrene), poly(vinyl chloride), poly(vinyl acetate) and poly(methyl methacrylate). Representative reactions belonging to the class of ionic polymerization, also widely referred to as *living polymerization*, are *cationic polymerization* or *anionic polymerization,* depending on the charge of the active center at the growing chain end. Unlike radical polymerization, where the chain growth period is short relative to the overall reaction time, polymers grown using ionic polymerization maintain chain growth throughout the duration of the reaction (due to the "living" nature of these polymers), until external agents such as alcohols are used to terminate the reaction.[1,3,4]

1.3 Anionic Polymerization

The living nature of ionic polymerization enables high degree of control over molar mass and results in low polymer *PDI*. Furthermore, several blocks of monomers can be attached one after the other to form block copolymers. There are mainly two types of living ionic polymerization, namely cationic and anionic polymerization. Cationic/anionic polymerization is initiated by a cation/anion that further propagates on the growing polymeric chain end as a carbocation/carbanion.

Anionic polymerization can be initiated by *organometallic initiators* such as *sec*-butyl lithium, or via *electron transfer initiation*, *e.g.* by using sodium napthalide as the initiator.[1,4] The degree of association of carbanion and its counter cation significantly affects the polymerization kinetics. Various reaction parameters such as the solvent, cation and temperature can lead to the ion pair to exist in the following different types: an associated cluster; a polarized, covalent bond; a contact ion pair; a solvent separated ion pair; and free ions.

In the absence of impurities and unless external reagents are added to terminate the reaction, such as alcohols, ideally no termination or chain transfer reaction mechanisms occur during anionic polymerization. Due to high initiation rate as compared to chain propagation rate, simultaneous and equal chain growth occurs with all polymer chains that stay active or "living" after consuming all available monomers in the system. These active chains then can act as macroinitiators for a chemically new monomer, such that block copolymers can be grown one block after another onto the same growing polymer.

Synthesis of poly(isoprene-*b*-styrene-*b*-(4-vinyl)pyridine):

Poly(isoprene-*b*-styrene-*b*-(4-vinyl)pyridine) (ISV) triblock terpolymer is synthesized using a sequential anionic polymerization technique. Throughout the process involving living anions, strict exclusion of oxygen, water and other contaminants containing protons is maintained using high vacuum Schlenk lines to prevent polymer termination and minimize side reactions. Figure 1.1 depicts the reaction mechanism involved in the polymerization of ISV. Benzene is cleaned and distilled into a reactor flask to act as a solvent. Then, in a glove box *sec*-butyl lithium is added to the reactor using a syringe. Distilled isoprene is then added to this reactor and is allowed to polymerize overnight, following which an aliquot is terminated with degassed methanol for gel-permeation chromatography (GPC) analysis. Then, distilled styrene is added to the reactor and is polymerized overnight. Once again, a GPC sample is extracted from the IS diblock solution for analysis and diphenylethylene (DPE) is subsequently added to the reactor flask and allowed to react with IS for 30 minutes. The benzene in the flask is then exchanged with equal amounts of tetrahydrofuran (THF) by distillation using the Schlenk line. Then the reactor is cooled to -78 °C and freshly distilled (4-vinyl)pyridine is added. The polymerization is carried out for 1.5 hours to form the triblock terpolymer, following which it is terminated using degassed methanol. The THF in the reactor flask is then removed and the final triblock terpolymer is dissolved in chloroform and precipitated into methanol.

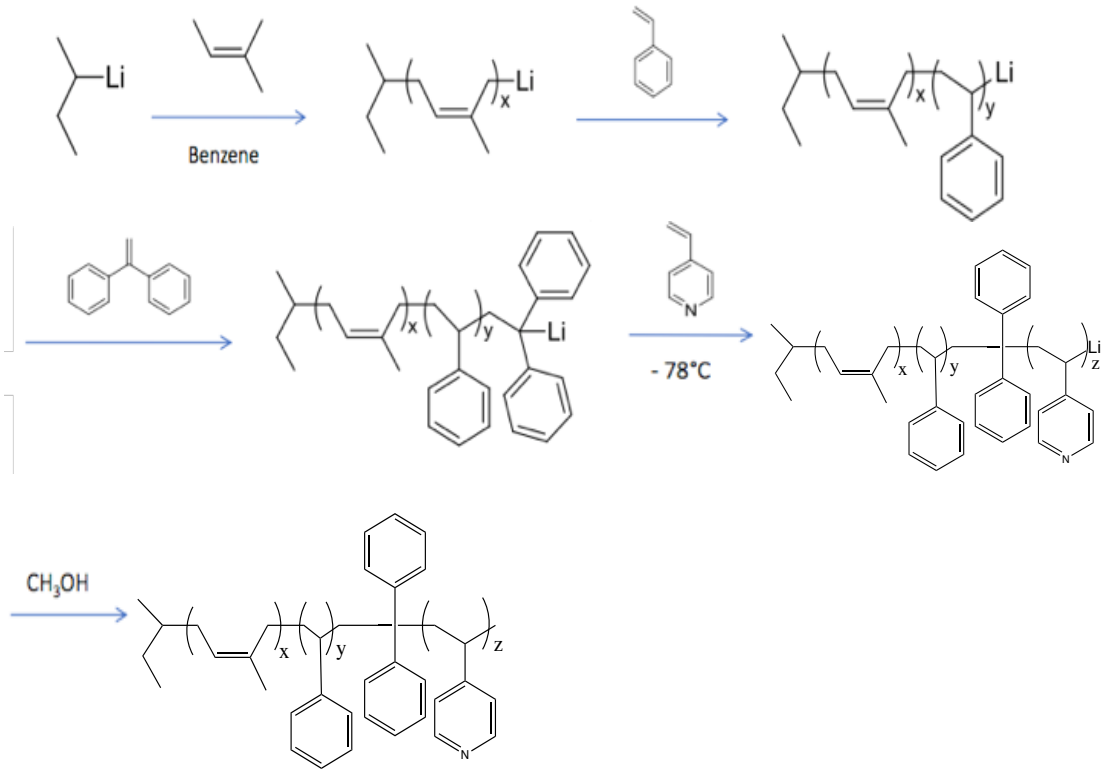

Figure 1.1. Anionic polymerization scheme of ISV triblock terpolymer.

Synthesis of poly(isoprene-*b*-styrene-*b*-ethyleneoxide):

Poly(isoprene-*b*-styrene-*b*-ethylene oxide) (ISO) triblock terpolymer is also synthesized using a sequential anionic polymerization technique as shown in Figure 1.2. The technique used to synthesize the IS diblock is the same as that described earlier for the ISV synthesis. However, instead of reaction with DPE, the living IS polymer chain is end-functionalized with an addition of excess ethylene oxide and is then terminated with methanolic hydrochloric acid. Since the ethylene oxide cannot self-polymerize with lithium as the counter ion, only end capping occurs by one ethylene oxide monomer unit per chain to form hydroxyl end-capped IS. After the end-capping process, multiple washing steps of the polymer solution is carried out

using sodium bicarbonate and deionized water. Thorough washing is required to flush out the lithium chloride formed during termination with methanolic hydrochloric acid. Following the removal of lithium chloride, a solvent exchange between benzene and THF is carried out and excess potassium chloride is added to the reactor. The hydroxyl end capped IS diblock copolymer is then reinitiated using potassium naphthalenide to form a potassium alkoxide chain end. This acts as a macroinitiator to polymerize ethylene oxide monomers using a ring opening polymerization mechanism. The ethylene oxide is allowed to polymerize for four days. After polymerization is complete, the reaction is once again terminated using methanolic hydrochloric acid. The THF in the reactor flask is then removed; the final triblock terpolymer is dissolved in chloroform and again washed several times to remove potassium chloride. Finally, the concentrated polymer solution in chloroform is precipitated out in methanol.

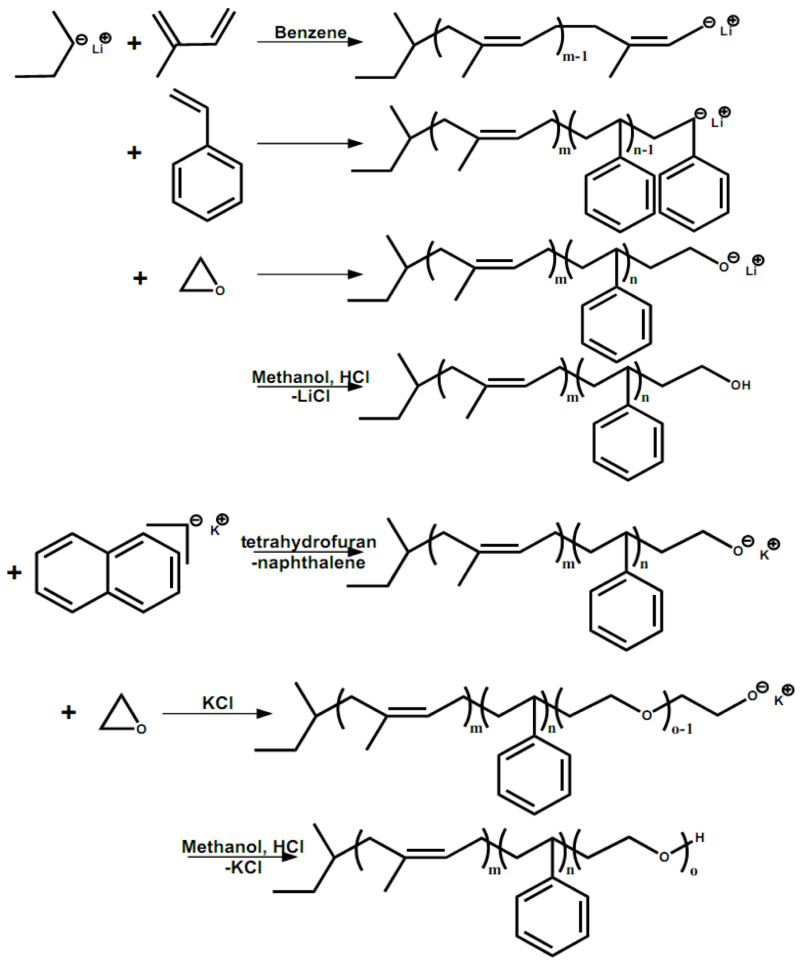

Figure 1.2. Anionic polymerization scheme of ISO triblock terpolymer.

1.4 Block Copolymer Self-Assembly

Block copolymers are macromolecules in which two or more homopolymer subunits are linked together by covalent bonds. Depending on the number of distinct blocks in such a macromolecule, they can be classified as diblock copolymers, triblock copolymers, triblock terpolymers, etc.

For a polymer mixture containing two polymers A and B, the mixing between the blocks can be described using change in the Gibbs free energy of mixing ΔG_m:

$$\frac{\Delta G_m}{k_b T} N = f_A \ln f_A + f_B \ln f_B + f_A f_B \chi_{AB} N \quad (1.4.1)$$

Where f_A and f_B are the volume fractions of polymers A and B in the mixture, *N* is the degree of polymerization, χ_{AB} is the Flory-Huggins interaction parameter [4,5] between A and B, k_b is the Boltzmann constant and T is the temperature. Polymer mixing is favored if the value of ΔG_m is negative and polymer phase separation is favored if ΔG_m is positive. The value of χ_{AB} can be calculated using the Hansen solubility parameters [6] employing the following equation:

$$\chi_{AB} = \frac{V_m}{k_b T} \left[(\delta_{dA} - \delta_{dB})^2 + 0.25 \left(\delta_{pA} - \delta_{pB} \right)^2 + 0.25 (\delta_{hA} - \delta_B)^2 \right] \quad (1.4.2)$$

where V_m is the molar volume, and δ_{di} is the dispersive, δ_{pi} is the polar, and δ_{hi} is the hydrogen bonding contributions of polymer *i* to the Hansen solubility parameter. The phase separation of polymer mixtures is favored when χ_{AB} is positive and the value of $\chi_{AB} N$ is sufficiently large.

Since the different polymer blocks are connected together by covalent bond, in block copolymers macrophase separation does not occur. To lower overall free energy by avoid unfavorable interactions, microphase separation between neighboring polymer

blocks occurs and leads to formation of periodic and ordered structures of self-assembled blocks on the length scale of around 5-100 nm.[7] During microphase separation, different morphologies can be formed depending on the values of f and χN. For diblock copolymers, typical morphologies observed as a function of block volume fraction, f, are close-packed spheres (CPS), spherical body-centered cubic micellar (S, Q^{229}), hexagonal cylinder (H), gyroidal (G, Q^{230}) or lamellar phases (L) as shown in Figure 1.3.[8]

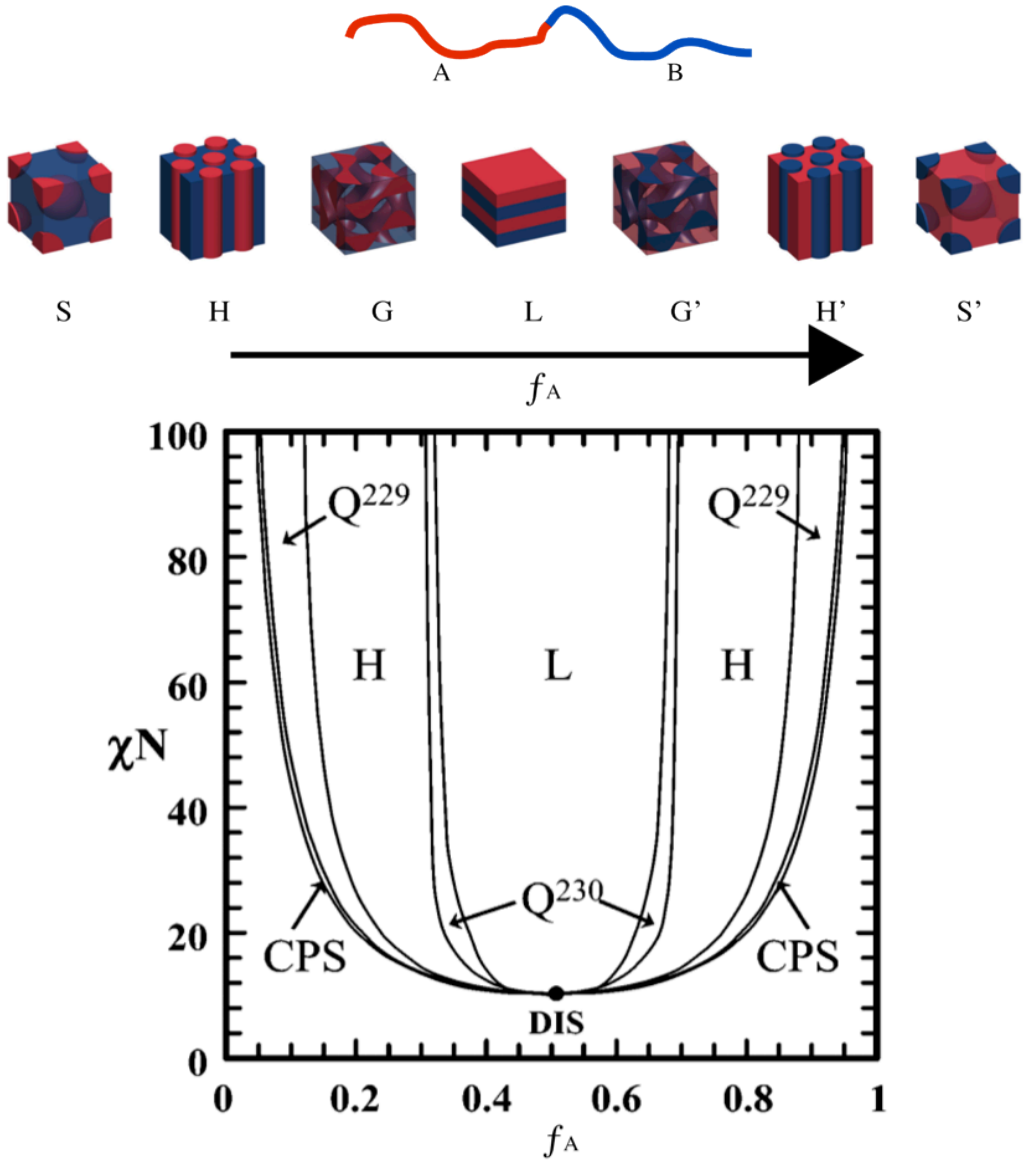

Figure 1.3. Top: Typical block copolymer morphologies observed during self-assembly of an A- B diblock copolymer.
Bottom: Equilibrium morphology diagram for a diblock copolymer as a function of f_A exhibiting spherical body-centered cubic micellar (S, Q^{229}), close-packed spheres (CPS), hexagonal cylinder (H), gyroidal (G, Q^{230}) and lamellar phases (L). [8]

For linear triblock terpolymer systems a larger variety of different self-assembled morphologies is observed. For example, extensive studies on the linear ABC triblock terpolymer system poly(isoprene-*b*-styrene-*b*-ethyleneoxide) have been

previously conducted. [9,10]

1.5 Non-Solvent Induced Phase Separation

The most commonly used technique to fabricate synthetic polymer based asymmetric ultrafiltration (UF) membranes is called non-solvent induced phase separation (NIPS), also referred to as phase inversion. To make a flat sheet membrane using NIPS, a polymer solution comprised of the polymer in an appropriate solvent system is blade casted onto a substrate, and then plunged into a coagulation bath consisting of a non-solvent for the polymer. On plunging the casted polymer film in the coagulation bath, the solvent and the non-solvent rapidly exchange leading to precipitation of the polymer and formation of the phase inverted membrane structure. There might be more than one polymer involved in the solution (called dope), and additives may be added either to the dope solution or to the coagulation bath.

If upon plunging of the polymer film into the coagulation bath solvent and non-solvent exchange rapidly, a finger-like membrane substructure results. Inversely, slow exchange of solvent and non-solvent leads to sponge-like membrane substructures as shown in Figure 1.4.[11] Hence, the selection of the polymer-solvent-precipitant system is very important as it dictates the final morphology of the membrane substructure fabricated using NIPS process.[12]

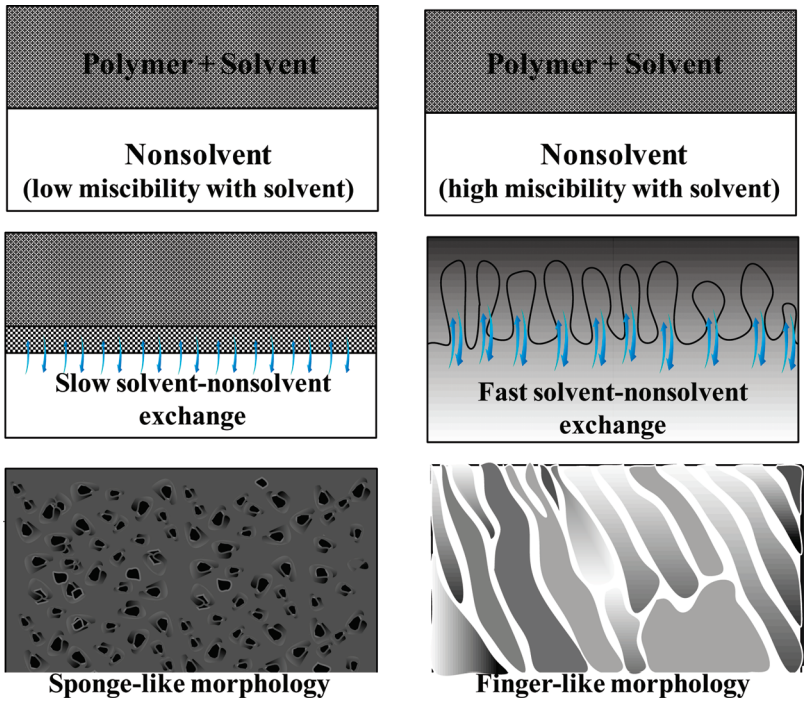

Figure 1.4. Various NIPS membrane substructures as a function of the rate of solvent and non-solvent exchange.[11]

1.6 SNIPS Procedure to Fabricate Block Copolymer derived Asymmetric UF Membranes

The process combining block copolymer self-assembly and non-solvent induced phase separation (SA + NIPS = SNIPS) to fabricate asymmetric polymer membranes was first introduced a decade ago by Peinemann *et al*.[13] They used poly(styrene-*b*-(4-vinyl)pyridine) (SV) to prepare asymmetric membranes that consisted of a surface top layer of 200-300 nm thickness with cylindrical pores aligned normal to the membrane surface, and a graded porous substructure. The primary advantage of membranes prepared using SNIPS technique is the combination of high pore densities with narrow pore size distributions leading to superior values of permeability and selectivity[14], also known as permselectivity, as compared to conventional UF membranes, making them highly desirable for applications such as ultrafiltration (UF), protein separation and drug-delivery.

The SNIPS procedure is illustrated in figure 1.5.[15] A thin film of block copolymer dope solution is casted onto a suitable substrate. This film is allowed to evaporate for a defined time period, during which the polymer concentration increases at the interface between the film and air leading to a solvent gradient along the film normal. This drives the block copolymer self-assembly process at the surface, following which the film is plunged into a non-solvent bath. Similar to NIPS, solvent and non-solvent exchange leads to precipitation of the polymer. The membranes formed using SNIPS technique usually depict an isoporous and ordered, selective skin layer of 100-200 nm thickness on top of an asymmetric macroporous sub-structure.

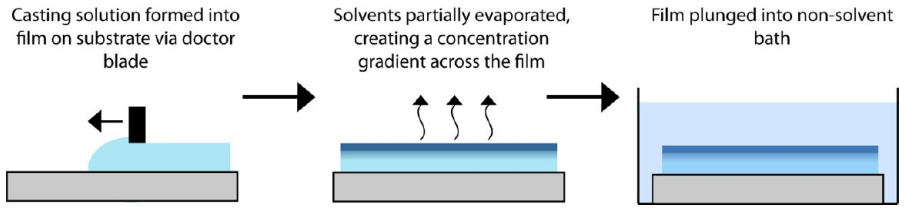

Figure 1.5. A schematic depicting the SNIPS procedure to fabricate membranes.[15]

Since its inception in 2007, the SNIPS technique has been extended to a variety of block copolymer systems. This includes diblock copolymers such as poly(styrene-*b*-(2-vinyl)pyridine)[16], poly(styrene-*b*-(4-vinyl)pyridine-N-oxide)[17] and poly(styrene-*b*-ethylene oxide).[18,19] Furthermore, a number of triblock terpolymer systems have also been explored such as poly(isoprene-*b*-styrene-*b*-(4-vinyl) pyridine) (ISV),[20] poly(isoprene-*b*-styrene-*b*-*N*,*N*-dimethylacrylamide),[21] and poly(styrene-*b*-4-vinylpyridine-*b*-propylene sulfide).[22]

There have been a number of studies aimed at controlling structure of the selective skin layer[23,24] as well as the underlying substructure[25] of asymmetric membranes fabricated using SNIPS process. Furthermore, small organic molecules,[26,27] and polymers,[28] have been added to the polymer dope solution to tune membrane properties such as pore size and pore size distribution. Finally, co-assembly and non-solvent induced phase separation (CNIPS) has been introduced to either prepare polymer organic-inorganic hybrid membranes by addition of either inorganic nanoparticles to the polymer dope[29], or carbon materials using phenol-formaldehyde resols.[30]

In parallel, in order to understand the underlying structure formation mechanisms of SNIPS process, techniques such as solution small-angle X-Ray scattering (SAXS)[31] and *in situ* grazing incidence small-angle X-Ray scattering (GISAXS)[32] have been previously applied.

1.7 Thesis outline

Membranes prepared using the SNIPS process have proven to be promising candidates for a variety of applications such as ultrafiltration, protein and nutraceutical separation, and drug-delivery. This is the result of the ability of these membranes to marry high permeability with superior selectivity, but is also based on potentially greater control over membrane structure and composition.

The phenomenon of biofouling commonly occurs during filtration processes and leads to undesirable consequences such as pore blockage and formation of a biofilm on the membrane surface. This degrades their permselectivity and results in a need to frequently clean or replace the membranes. Previous studies have indicated that SNIPS membranes in which 4-vinylpyridine chains decorate the pore walls are prone to fouling by proteins.[33]

Thus, improved systems are highly desirable that incorporate an anti-fouling property on the surface of the membranes while retaining the high performance capabilities of SNIPS membranes. Poly(ethylene oxide) (PEO) is a promising candidate block to reduce membrane fouling due to its hydrophilic nature. Chapter 2 of this thesis explores an attempt to extend the SNIPS process to a new polymer with PEO end block, poly(isoprene-*b*-styrene-*b*-ethylene oxide) (ISO). Various membrane formation parameters such as solvent system, polymer dope concentration, evaporation time, coagulation bath, *etc*. are explored to optimize ISO SNIPS membranes to obtain desired structure and performance. Current results prove this attempt to be largely unsuccessful, and further optimization is required before competitive pure ISO SNIPS membranes can be fabricated.

To overcome this impediment, as described in Chapter 3 two chemically distinct triblock terpolymers, poly(isoprene-*b*-styrene-*b*-(4-vinyl) pyridine) (ISV) and ISO are subsequently blended in the dope solution in order to fabricate membranes using the SNIPS process. The morphology, pH-dependent permeability and protein adsorption resistance of the blended membranes are characterized. The merits, limitations and opportunities of this "mix and match" blending approach are discussed.

1.8 References

1. Young, R. J.; Lovell P. A. *Introduction to polymers*. CRC press, 2011.
2. Carothers, W. H. Studies on polymerization and ring formation. I. An introduction to the general theory of condensation polymers. *J. Am. Chem. Soc.* **1929**, 51 (8), 2548–2559.
3. Odian, G. *Principles of polymerization*. John Wiley & Sons, 2004.
4. Flory, P. J. *Principles of polymer chemistry*. Cornell University Press, 1953.
5. Strobl, G. *The Physics of Polymers*; 3rd ed.; Springer-Verlag: Berlin Heidelberg, 2007.
6. Hansen, C. M., *Hansen Solubility Parameters: A User's Handbook*. 2nd ed.; CRC Press: Boca Raton, FL, 2007.
7. Matsen, M. W. The standard Gaussian model for block copolymer melts. *J. Phys. Condens. Matter* **2001**, 14 (2).
8. Cochran, E. W.; Garcia-Cervera, C. J.; Fredrickson, G. H. Stability of the gyroid phase in diblock copolymers at strong segregation. *Macromolecules* **2006**, 39 (7), 2449–2451.
9. Chatterjee, J.; Jain, S.; Bates, F. S. Comprehensive phase behavior of poly (isoprene-b-styrene-b-ethylene oxide) triblock copolymers. *Macromolecules* **2007**, 40 (8), 2882–2896.
10. Epps, T. H.; Cochran, E. W.; Bailey, T. S.; Waletzko, R. S.; Hardy, C. M.; Bates, F. S. Ordered network phases in linear poly (isoprene-b-styrene-b-ethylene oxide) triblock copolymers. *Macromolecules* **2004**, 37 (22), 8325–8341.

11. Guillen, G. R.; Pan, Y.; Li, M.; Hoek, E. M. V. Preparation and characterization of membranes formed by nonsolvent induced phase separation: a review. *Ind. Eng. Chem. Res.* **2011**, 50 (7), 3798–3817.
12. Strathmann, H.; Kock, K. The formation mechanism of phase inversion membranes. *Desalination* **1977**, 21 (3), 241–255.
13. Peinemann, K.V.; Abetz, V.; Simon, P. F. W. Asymmetric superstructure formed in a block copolymer via phase separation. *Nat. Mater.* **2007**, 6 (12), 992–996.
14. Pendergast, M. M.; Dorin, R. M.; Phillip, W. A.; Wiesner, U.; Hoek, E. M. Understanding the structure and performance of self-assembled triblock terpolymer membranes. *J. Membr. Sci.* **2013**, 444, 461–468.
15. Dorin, R. M.; Sai, H.; Wiesner, U. Hierarchically porous materials from block copolymers. *Chem. Mater.* **2014**, 26 (1), 339–347.
16. Jung, A.; Rangou, S.; Abetz, C.; Filiz, V.; Abetz, V. Structure Formation of Integral Asymmetric Composite Membranes of Polystyrene-block-Poly (2-vinylpyridine) on a Nonwoven. *Macromol. Mater. Eng.* **2012**, 297 (8), 790–798.
17. Shevate, R.; Karunakaran, M.; Kumar, M.; Peinemann, K.V. Polyanionic pH-responsive polystyrene-b-poly (4-vinyl pyridine-N-oxide) isoporous membranes. *J. Membr. Sci.* **2016**, 501, 161–168.
18. Hahn, J.; Filiz, V.; Rangou, S.; Clodt, J.; Jung, A.; Buhr, K.; Abetz, C.; Abetz, V. Structure formation of integral-asymmetric membranes of

polystyrene-block-poly (ethylene oxide). *J. Polym. Sci., Part B: Polym. Phys.* **2012**, 51 (4), 281–290.

19. Karunakaran, M.; Nunes, S. P.; Qiu, X.; Yu, H.; Peinemann, K.V. Isoporous PS-b-PEO ultrafiltration membranes via self-assembly and water-induced phase separation. *J. Membr. Sci.* **2014**, 453, 471–477.
20. Phillip, W. A.; Dorin, R. M.; Werner, J.; Hoek, E. M. V.; Wiesner, U.; Elimelech, M. Tuning structure and properties of graded triblock terpolymer-based mesoporous and hybrid films. *Nano Lett.* **2011**, 11 (7), 2892–2900.
21. Mulvenna, R. A.; Weidman, J. L.; Jing, B.; Pople, J. A.; Zhu, Y.; Boudouris, B. W.; Phillip, W. A. Tunable nanoporous membranes with chemically-tailored pore walls from triblock polymer templates. *J. Membr. Sci.* **2014**, 470, 246–256.
22. Zhang, Q.; Gu, Y.; Li, Y. M.; Beaucage, P. A.; Kao, T.; Wiesner, U. Dynamically responsive multifunctional asymmetric triblock terpolymer membranes with intrinsic binding sites for covalent molecule attachment. *Chem. Mater.* **2016**, 28 (11), 3870–3876.
23. Dorin, R. M.; Phillip, W. A.; Sai, H.; Werner, J.; Elimelech, M.; Wiesner, U. Designing block copolymer architectures for targeted membrane performance. *Polymer* **2014**, 55 (1), 347–353.
24. Rangou, S.; Buhr, K.; Filiz, V.; Clodt, J. I.; Lademann, B.; Hahn, J.; Jung, A.; Abetz, V. Self-organized isoporous membranes with tailored pore sizes. *J. Membr. Sci.* **2014**, 451, 266–275.
25. Zhang, Q.; Li, Y. M.; Gu, Y.; Dorin, R. M.; Wiesner, U. Tuning substructure

and properties of supported asymmetric triblock terpolymer membranes. *Polymer* **2016**, 107, 398–405.

26. Clodt, J. I.; Rangou, S.; Schröder, A.; Buhr, K.; Hahn, J.; Jung, A.; Filiz, V.; Abetz, V. Carbohydrates as additives for the formation of isoporous PS-b-P4VP diblock copolymer membranes. *Macromol. Rapid Commun.* **2012**, 34 (2), 190–194.
27. Gu, Y.; Wiesner, U. Tailoring pore size of graded mesoporous block copolymer membranes: moving from ultrafiltration toward nanofiltration. *Macromolecules* **2015**, 48 (17), 6153–6159.
28. Radjabian, M.; Abetz, V. Tailored pore sizes in integral asymmetric membranes formed by blends of block copolymers. *Adv. Mater.* **2014**, 27 (2), 352–355.
29. Gu, Y.; Dorin, R. M.; Wiesner, U. Asymmetric organic–inorganic hybrid membrane formation via block copolymer–nanoparticle co-assembly. *Nano Lett.* **2013**, 13 (11), 5323–5328.
30. Hesse, S. A.; Werner, J. G.; Wiesner, U. One-Pot Synthesis of Hierarchically Macro-and Mesoporous Carbon Materials with Graded Porosity. *ACS Macro Lett.* **2015**, 4 (5), 477–482.
31. Dorin, R. M.; Marques, D. S.; Sai, H.; Vainio, U.; Phillip, W. A.; Peinemann, K.-V.; Nunes, S. P.; Wiesner, U. Solution small-angle X-ray scattering as a screening and predictive tool in the fabrication of asymmetric block copolymer membranes. *ACS Macro Lett.* **2012**, 1 (5), 614–617.
32. Gu, Y.; Dorin, R. M.; Tan, K. W.; Smilgies, D. M.; Wiesner, U. In situ study

of evaporation-induced surface structure evolution in asymmetric triblock terpolymer membranes. *Macromolecules* **2016**, 49 (11), 4195–4201.

33. Hahn, J.; Clodt, J. I.; Filiz, V.; Abetz, V. Protein separation performance of self-assembled block copolymer membranes. *RSC Adv.* **2014**, 4 (20), 10252.

CHAPTER 2

Optimization of poly(isoprene-*b*-styrene-*b*-ethylene oxide) membranes produced using the SNIPS process

2.1 Abstract

Poly(isoprene-*b*-styrene-*b*-ethylene oxide) (ISO) was used to fabricate membranes using the block copolymer self-assembly and non-solvent induced phase separation (SNIPS) process. Various concentrations of the dope solution in two solvent systems, 7:3 DOX/THF and 6:3:1 DMF/THF/DOX (by weight), were investigated using solution small-angle X-ray scattering **(**SAXS). Polymer dope solutions for both these solvent systems show ordering into a body-centered cubic (BCC) lattice at higher polymer concentrations. Membranes were prepared using the above solvent systems and various coagulation baths. Scanning electron microscopy (SEM) analysis of these membranes reveals morphologies not conducive to high permselectivity. This study reveals challenges in SNIPS formation of a pure ISO-based asymmetric membrane and the need to explore alternative strategies such as blending to overcome this predicament.

Keywords: triblock terpolymer, self-assembly, SNIPS, asymmetric membranes

2.2 Introduction

There is a growing interest in membranes prepared using block copolymer self-assembly and non-solvent induced phase separation (SNIPS)[1] process, due to their superior permselectivities compared to commercial ultrafiltration membranes.[2] Peinemann *et al.* prepared the first SNIPS membrane using a diblock copolymer poly(styrene-*b*-(4-vinyl)pyridine).[3] Since its introduction, a variety of diblock copolymer and triblock terpolymer systems such as poly(styrene-*b*-(2-vinyl)pyridine)[4] and poly(isoprene-*b*-styrene-*b*-(4-vinyl) pyridine)[5] (ISV) have been explored to fabricate membranes using the SNIPS process.

Membranes from block copolymers such as poly(styrene-*b*-(4-vinyl) pyridine) in which (4-vinyl)pyridine (4VP) blocks decorate the pore walls have previously shown high protein adsorption behavior.[6] This is undesirable due to a higher susceptibility to biofouling. Biofouling is an unfavorable phenomenon during membrane usage which leads to reduction in pore size, pore blockage and formation of a biofilm on the membrane surface.[7] Hence, there is a need to couple the high permselectivities of SNIPS membranes with favorable antifouling properties of the pore surfaces. The hydrophilic nature of poly(ethylene oxide) (PEO) has been widely exploited to reduce fouling behavior of membranes. To that end, there have been several attempts to fabricate block copolymer SNIPS membranes containing PEO as one of the blocks. For example, recently poly(styrene-*b*-ethylene oxide)[8,9] and poly(styrene-*b*-2-vinylpyridine-*b*-ethylene oxide)[10] membranes have been fabricated using SNIPS process.

In this study we explore a new polymer system, poly(isoprene-*b*-styrene-*b*-ethylene oxide) (ISO), for fabrication of SNIPS membranes. Extending the SNIPS process to a new polymer system involves an extensive optimization process over a multitude of parameters. Several solvent systems, concentrations, evaporation times and non-solvents are explored via systematic parameter variations. Although a pure ISO derived SNIPS membrane with desired structure and properties still remains a challenge, this study provides the motivation for an alternative "mix and match" approach described in Chapter 3 to overcome the challenges of working with pure ISO.

2.3 Experimental Methods

2.3.1 Polymer Synthesis and Characterization

The triblock terpolymer poly(isoprene-*b*-styrene-*b*-ethyleneoxide) (ISO) used in this study was prepared using sequential anionic polymerization technique as described in Chapter 1. The molar masses (M_n) and volume fractions of polymer blocks (f) of the synthesized ISO was determined using a combination of gel permeation chromatography (GPC) and ^{1}H NMR. A summary of the ISO triblock terpolymer characterization results is shown in Table 2.1.

Table 2.1. Number average molar mass (M_n), volume fraction (f), and polydispersity index (PDI) of the ISO used in this study.

Polymer	M_n (kg/mol)	f_{PI}	f_{PS}	f	PDI
ISO	154	0.24	0.67	0.09	1.07

2.3.2 Small-angle X-Ray scattering (SAXS)

The block copolymer solutions for SAXS analysis were prepared by dissolving the ISO at various concentrations in different solvent systems involving solvents such as 1,4-dioxane (DOX), tetrahydrofuran (THF) and dimethylformamide (DMF). Solvent systems were prepared by mixing solvents in ratios such as 7:3 DOX/THF and 6:3:1 DMF/THF/DOX (by weight), prior to adding ISO. Polymer solutions were injected into 1mm capillaries using a syringe. The capillaries were sealed using epoxy glue before SAXS experiments were performed.

SAXS measurements were performed on the G1 beamline at the Cornell High Energy Synchrotron Source (CHESS). If θ is one-half value of the scattering angle, the scattering vector, q, is described using the following equation:

$$q = \frac{4\pi}{\lambda} sin\theta \quad (2.2.2)$$

2.3.3 Membrane Fabrication and Characterization

The ISO membranes were fabricated using the SNIPS process. 18% of ISO dissolved in the appropriate solvent system, 7:3 DOX/THF or 6:3:1 DMF/THF/DOX (by weight) was used as the polymer dope. A thin film with thickness between 203 μm and 229 μm of the dope solution was casted onto a glass substrate using an automated blade-casting machine. The solvents were evaporated for a set period of time to drive the block copolymer self-assembly process. Finally, the film was precipitated in the appropriate coagulation bath such as deionized water for 7:3 DOX/THF solvent and cold diethylether (DEE) and hexanes in case of 6:3:1 DMF/THF/DOX solvent. The lower than room temperature conditions (1 °C to 4 °C) of DEE were maintained by cooling using an ice-bath.

Scanning Electron Microscopy (SEM) micrographs were obtained using a Tescan Mira3 field emission scanning electron microscope (FE-SEM) at an acceleration voltage of 5 kV and a working distance of 3-5 mm. The membrane samples were dried and sputter coated with gold-palladium using a Denton Vacuum Desk II for 8 seconds prior to imaging.

2.4 Results and Discussion

2.4.1 Small-angle X-Ray scattering (SAXS) analysis

The SAXS curves obtained for the ISO dope solutions at different concentrations in two different solvent systems, 7:3 DOX/THF or 6:3:1 DMF/THF/DOX, are shown in Figure 2.1. The dashed markings correspond to expected peak positions for a BCC lattice with lattice constants of 48.2 nm for (a) and 48.8 nm for (b).

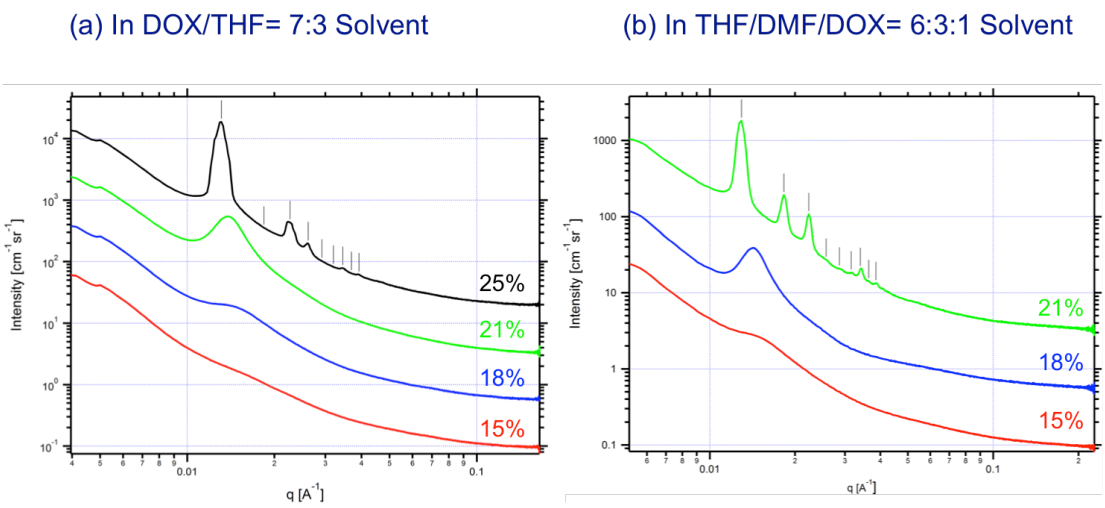

Figure 2.1. Small-angle X-Ray scattering curves for ISO at varying polymer concentrations in (a) 7:3 wt% DOX/THF and (b) 6:3:1 wt% DMF/THF/DOX.

In both solvent systems the ISO evolved from a disordered structure at low polymer concentrations to an ordered structure consistent with a BCC lattice at higher concentrations, *i.e.* 25% in 7:3 wt% DOX/THF and 21% in 6:3:1 wt% DMF/THF/DOX.

Previous studies have suggested that membranes cast using SNIPS from solutions that have concentrations slightly below the on-set of ordering in SAXS patterns lead to block copolymer membranes with well defined surface structures.[11] In the current work, ISO dissolved in both the above solvent systems show order in solution SAXS suggesting that well-ordered asymmetric membranes using SNIPS might be accessible.

2.4.2 Membrane Characterization

The ISO membranes were prepared using the SNIPS process by plunging the above-mentioned thin films using the two solvent systems in various non-solvents. Deionized water was used as a coagulation bath for 7:3 DOX/THF solvent, and cold diethylether (DEE) and hexanes were used in case of 6:3:1 DMF/THF/DOX solvent. The evaporation times prior to plunging in non-solvent for the above-mentioned systems were 80 seconds, 80 seconds and 160 seconds, respectively. The SEM images of the top and bottom surfaces as well as the cross-section of the various membranes obtained are depicted in Figure 2.2.

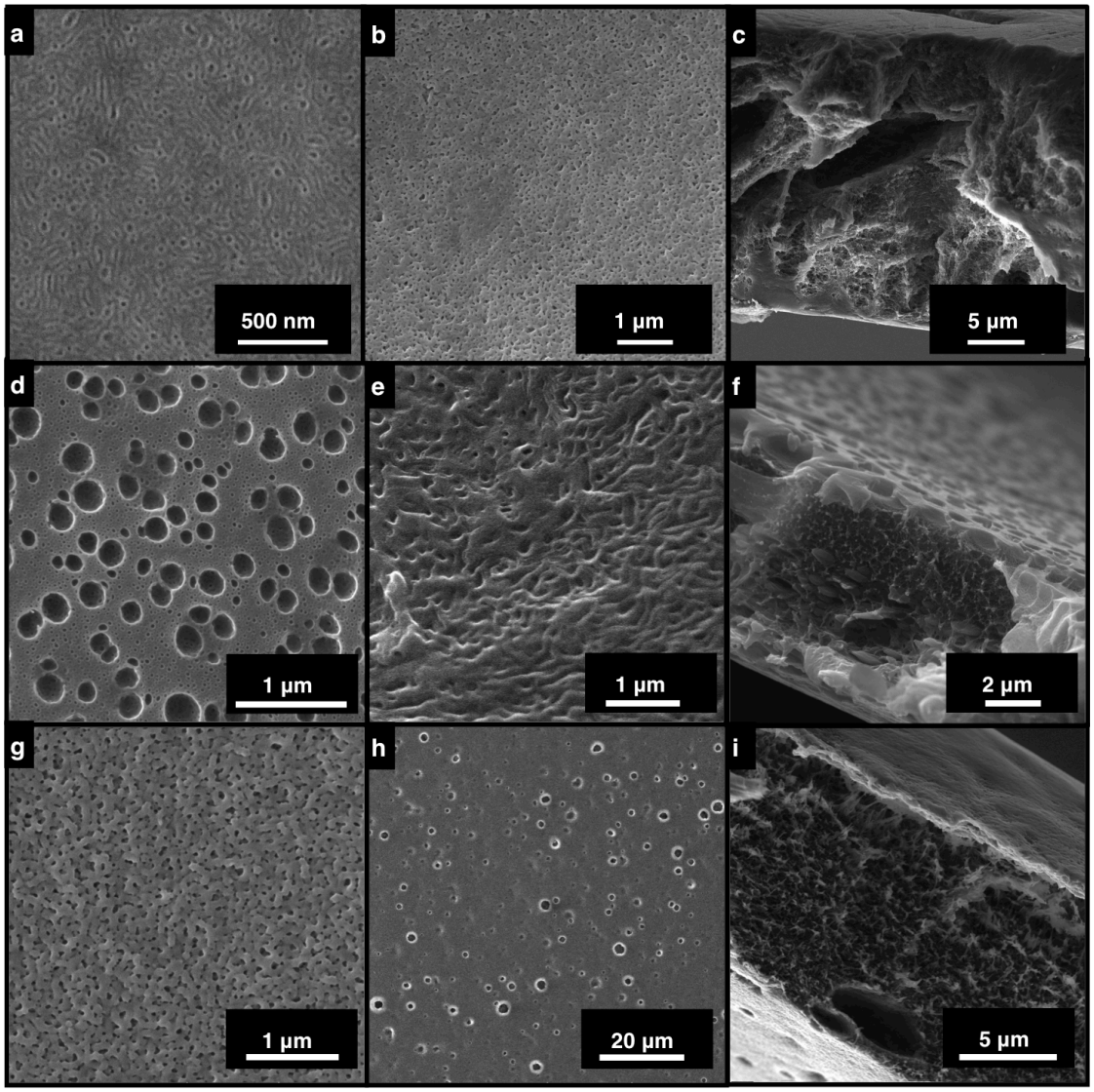

Figure 2.2. SEM micrographs of ISO membranes. Top surfaces (first column), bottom surfaces (second column), and cross-sectional images (third column) of membranes fabricated using (a-c) 18% ISO in 7:3 DOX/THF solvent and deionized water as non-solvent, (d-e) 18% ISO 6:3:1 DMF/THF/DOX solvent and cold DEE as non-solvent, and (g-f) 18% ISO 6:3:1 DMF/THF/DOX solvent and hexanes as non-solvent. Since the system in cold DEE non-solvent was not consistently reproducible, (d-e) are representative images of samples in majority of the trials.

For 18% ISO in 7:3 DOX/THF solvent and deionized water as non-solvent, as shown in figure 2.2 (a) it is observed that the pores on the top surface appear closed and the surface appears disordered, in (b) the bottom surface appears to lack porosity,

and the cross-section in (c) depicts a dense spongy substructure of the membrane. Such membrane morphology is likely to depict poor permselectivity. Furthermore, large area samples made using this system consistently showed macroscopic defects (see Appendix Figure A.1 (a)).

In the case of 18% ISO 6:3:1 DMF/THF/DOX solvent and cold DEE as non-solvent, as shown in figure 2.2 (d) the top surface of the membrane shows the presence of large macroscopic defects alongside isoporous circular pores. Once again, such a membrane is likely to exhibit inferior permselectivity. Several efforts to minimize these macroscopic defects were rendered unsuccessful, likely due to the limited control over moisture absorption into the cold DEE coagulation bath.

The third system of 18% ISO 6:3:1 DMF/THF/DOX solvent and hexanes as non-solvent, as shown in figure 2.2 (g), depicts the presence of relatively isoporous pores despite an absence of pore ordering. Figure 2.2 (h) and (i) show the limited presence of pores and a dense spongy substructure, respectively. Large, translucent defect-free membrane samples could be prepared using this system as shown in Appendix Figure A.1 (b). Permeability tests were performed using these membranes, and very low values of normalized flux values (~50 LMH/bar) were obtained.

2.5 Conclusion

The SNIPS process requires control over a variety of parameters such as solvent system, concentration, non-solvent, evaporation time, substrate, *etc.* in order to fabricate membranes that portray the desired structure and properties. Some of these parameters were explored for optimization of ISO SNIPS membranes, which proved to be largely unsuccessful. This study suggests the need to use other methods such as blending multiple block copolymers in the dope solution in order to fabricate SNIPS membranes containing PEO functionality.

Acknowledgements

P.N.V acknowledges the funding of this project by Contract No. HDTRA1-13-C0003 from the Defense Threat Reduction Agency (DTRA). This work utilized the facilities provided by the Cornell Center for Materials Research (CCMR) supported by NSF MRSEC program (DMR-1120296) and CHESS supported by the NSF & NIH/NIGMS via NSF award DMR-0936384. P.N.V thanks Q. Zhang and F. Matsuoka from the Wiesner group for help in the block copolymer synthesis.

2.6 Appendix A

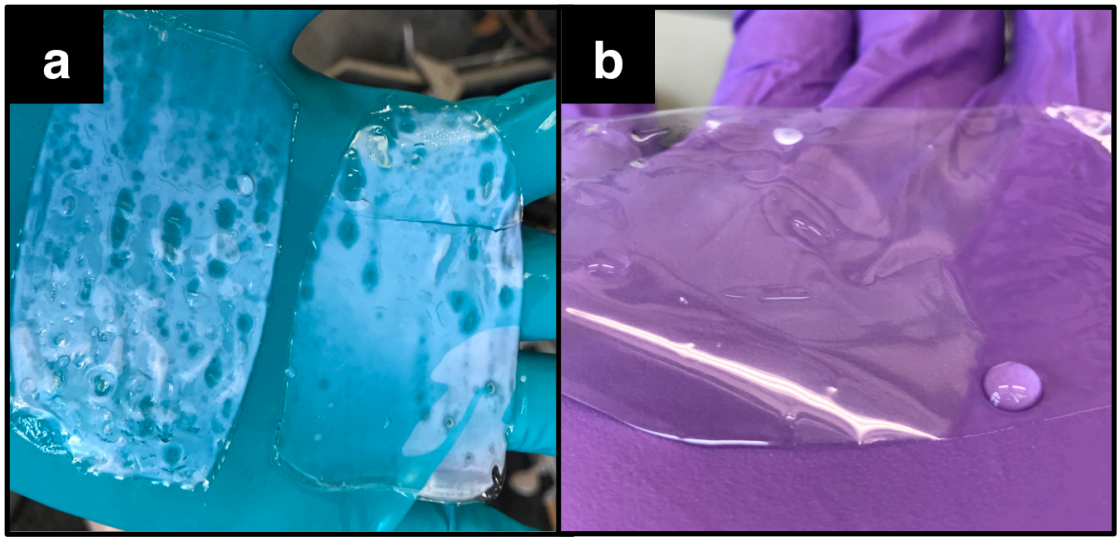

Figure A.1. Photographs of membranes prepared using (a) 18% ISO in 7:3 DOX/THF solvent and deionized water as non-solvent and (b) 18% ISO 6:3:1 DMF/THF/DOX solvent and hexanes.

2.7 References

1. Dorin, R. M.; Marques, D. S.; Sai, H.; Vainio, U.; Phillip, W. A.; Peinemann, K.V.; Nunes, S. P.; Wiesner, U. Solution Small-Angle X-ray Scattering as a Screening and Predictive Tool in the Fabrication of Asymmetric Block Copolymer Membranes. *ACS Macro Lett.* **2012**, 1 (5), 614–617.
2. Pendergast, M. M.; Dorin, R. M.; Phillip, W. A.; Wiesner, U.; Hoek, E. M. Understanding the structure and performance of self-assembled triblock terpolymer membranes. *J. Membr. Sci.* **2013**, 444, 461–468.
3. Peinemann, K.V.; Abetz, V.; Simon, P. F. W. Asymmetric superstructure formed in a block copolymer via phase separation. *Nat. Mater.* **2007**, 6 (12), 992–996.
4. Jung, A.; Rangou, S.; Abetz, C.; Filiz, V.; Abetz, V. Structure Formation of Integral Asymmetric Composite Membranes of Polystyrene-block-Poly (2-vinylpyridine) on a Nonwoven. *Macromol. Mater. Eng.* **2012**, 297 (8), 790–798.
5. Phillip, W. A.; Dorin, R. M.; Werner, J.; Hoek, E. M. V.; Wiesner, U.; Elimelech, M. Tuning structure and properties of graded triblock terpolymer-based mesoporous and hybrid films. *Nano Lett.* **2011**, 11 (7), 2892–2900.
6. Hahn, J.; Clodt, J. I.; Filiz, V.; Abetz, V. Protein separation performance of self-assembled block copolymer membranes. *RSC Adv.* **2014**, 4 (20), 10252.
7. Rana, D.; Matsuura, T. Surface modifications for antifouling membranes. *Chem. Rev.* **2010**, 110 (4), 2448–2471.

8. Hahn, J.; Filiz, V.; Rangou, S.; Clodt, J.; Jung, A.; Buhr, K.; Abetz, C.; Abetz, V. Structure formation of integral-asymmetric membranes of polystyrene-block-Poly (ethylene oxide). *J. Polym. Sci., Part B: Polym. Phys.* **2012**, 51 (4), 281–290.
9. Karunakaran, M.; Nunes, S. P.; Qiu, X.; Yu, H.; Peinemann, K.V. Isoporous PS-b-PEO ultrafiltration membranes via self-assembly and water-induced phase separation. *J. Membr. Sci.* **2014**, 453, 471–477.
10. Jung, A.; Filiz, V.; Rangou, S.; Buhr, K.; Merten, P.; Hahn, J.; Clodt, J.; Abetz, C.; Abetz, V. Formation of integral asymmetric membranes of AB diblock and ABC triblock copolymers by phase inversion. *Macromol. Rapid Commun.* **2013**, 34 (7), 610–615.
11. Dorin, R. M.; Marques, D. S.; Sai, H.; Vainio, U.; Phillip, W. A.; Peinemann, K.V.; Nunes, S. P.; Wiesner, U. Solution small-angle X-ray scattering as a screening and predictive tool in the fabrication of asymmetric block copolymer membranes. *ACS Macro Lett.* **2012**, 1 (5), 614–617.

CHAPTER 3

pH-responsive asymmetric membranes with anti-fouling properties derived from two chemically discrete triblock terpolymers blended during the SNIPS process

3.1 Abstract

Two chemically distinct triblock terpolymers, poly(isoprene-*b*-styrene-*b*-(4-vinyl) pyridine) (ISV) and poly(isoprene-*b*-styrene-*b*-ethylene oxide) (ISO), were blended in the dope solution in order to fabricate asymmetric membranes using block copolymer self-assembly and non-solvent induced phase separation (SNIPS) process. The ratios of ISV and ISO in the blended solutions were varied by weight. Both the pure ISV and the blended membranes exhibit a mesoporous skin layer atop a macroporous substructure. The asymmetric membranes from 9:1 and 7:3 ISV:ISO blends retained their pH-responsive permeability behavior characteristic for pure ISV membranes. Additionally, about a three-fold decrease in protein adsorption was observed in 5:5 blended membranes compared to pure ISV. Thus, the blended membranes exhibit properties characteristic of the chemistries present in both the parent block copolymers allowing two functionalities to be incorporated into a single membrane through the simple "mixing and matching" approach during the standard membrane fabrication process. Furthermore, the relative ratios of the parent block copolymers in the blend enable the tuning of properties of the resultant membranes. This study corroborates the ability and ease of the SNIPS process combined with the facile "mix and match" approach to access and tailor unique chemical functionalities in a single membrane opening doors to previously challenging applications.

Keywords: triblock terpolymer, self-assembly, SNIPS, asymmetric membranes, blending, anti-fouling

3.2 Introduction

First introduced by Pienemann *et al.*[1] a decade ago, membranes prepared using block copolymer self-assembly and non-solvent induced phase separation (SNIPS)[2] process have become increasingly desirable candidates for water purification and protein separation applications. These integral-asymmetric membranes, which exhibit an ordered isoporous top surface and a macroporous underlying substructure, are able to deliver higher permeabilities and superior selectivities when compared to traditional ultrafiltration membranes.[3] Moreover, the facile SNIPS technique offers a high degree of control over both the mesoporous skin layer and the underlying graded substructure. For example, the pore size of the selective top layer of SNIPS membranes have been tailored by changing the block copolymer molar mass,[4,5] using organic additives,[6] or forming binary blends from the same block copolymer varying in composition.[7] In another study, the cross-sectional morphology of membranes was tuned by varying parameters such as polymer solution concentration, evaporation time, and temperature of the non-solvent bath.[8] The most extensively studied system is that of the diblock copolymer poly(styrene-*b*-(4-vinyl)pyridine).[9-13] However, some other diblock copolymer systems such as poly(styrene-*b*-(2-vinyl)pyridine)[14] and poly(styrene-*b*-(4-vinyl)pyridine-N-oxide)[15] have been previously explored. The SNIPS process has also been extended to a variety of triblock terpolymer systems such as poly(isoprene-*b*-styrene-*b*-(4-vinyl) pyridine) (ISV),[16] poly(isoprene-*b*-styrene-*b*-*N*,*N*-dimethylacrylamide),[17] and poly(styrene-*b*-4-vinylpyridine-*b*-propylene sulfide).[18]

A major problem encountered in filtration processes is membrane fouling. Previous studies have suggested a high tendency of protein adsorption onto the surface

of SV membranes which have 4-vinylpyridine chains decorating the pore walls.[19] The resulting biofouling may lead to a variety of undesirable consequences such as reduction in surface porosity and effective pore size from pore blockage and formation of a biofilm on the surface.[20] These could translate into poor permselectivity and the need to frequently clean or replace membranes greatly limiting their use for protein separation and biopharmaceutical applications. Thus, there is a pressing need to design systems that incorporate an anti-fouling property while retaining the high performance capabilities of SNIPS membranes.

Poly(ethylene oxide) (PEO) has been widely used to reduce the fouling behavior of membranes which is attributed to the hydrophilic nature of PEO. Moreover, the water solubility and inherent biocompatibility of PEO makes it highly attractive for biomedical applications. Various strategies such as grafting[21,22] and incorporation as additives[23,24] have been used to introduce PEO into membranes. Additionally, there have been recent efforts to fabricate SNIPS membranes with block copolymers containing a PEO block such as in poly(styrene-*b*-ethylene oxide).[25,26] Another work used an ABC triblock terpolymer system, poly(styrene-*b*-2-vinylpyridine-*b*-ethylene oxide), to fabricate pH-responsive self-assembled asymmetric membranes that showed improved hydrophilicity.[27]

The extension of the SNIPS process to newly synthesized block copolymers is a challenging process as it involves optimizing a multitude of parameters to determine preparation conditions for the membranes. Therefore, it has been a challenging task to prepare poly(isoprene-*b*-styrene-*b*-ethylene oxide) (ISO) antifouling membranes using traditional SNIPS process that display an ordered isoporous top structure and exhibit

excellent membrane performance. One way to mitigate this problem is to employ a facile "mix and match" blending approach to circumvent the requirement of a standalone ISO membrane, while introducing the desired antifouling behavior of PEO. To that end, in a recent study two chemically distinct triblock terpolymer systems, namely ISV and poly(isoprene-*b*-styrene-*b*-(dimethylamino) ethyl methacrylate) (ISA), were blended in the casting solution to tailor the pH-responsive permeabilities of the resultant membranes.[28] This proved to be a promising way to introduce and modify distinct chemical functionalities in a single membrane.

In this study, we demonstrate the ability to blend ISV and ISO during the membrane fabrication process to prepare blended membranes with pH-responsiveness and tunable protein adsorption behavior. This blending approach applied during the SNIPS process proves to be an effective tool to access unique chemical functionalities to fabricate highly engineered membranes.

3.3 Experimental Methods

3.3.1 Polymer Synthesis and Characterization

The triblock terpolymers poly(isoprene-*b*-styrene-*b*-(4-vinyl)pyridine) (ISV) and poly(isoprene-*b*-styrene-*b*-ethyleneoxide) (ISO) used in this study were prepared using sequential anionic polymerization technique as described previously.[16,29] The synthesized ISV and ISO have similar molar mass (M_n) and volume fractions of polymer blocks (f), which were determined using a combination of gel permeation chromatography (GPC) and ^{1}H NMR. A summary of triblock terpolymer characterization results is shown for both terpolymers in Table 3.1.

Table 3.1. Number average molar mass (M_n), volume fraction (f), and polydispersity index (PDI) of the triblock terpolymers used in this study.

Terpolymer	M_n (kg/mol)	f_{PI}	f_{PS}	f	PDI
ISV	164	0.25	0.65	0.10	1.17
ISO	154	0.24	0.67	0.09	1.07

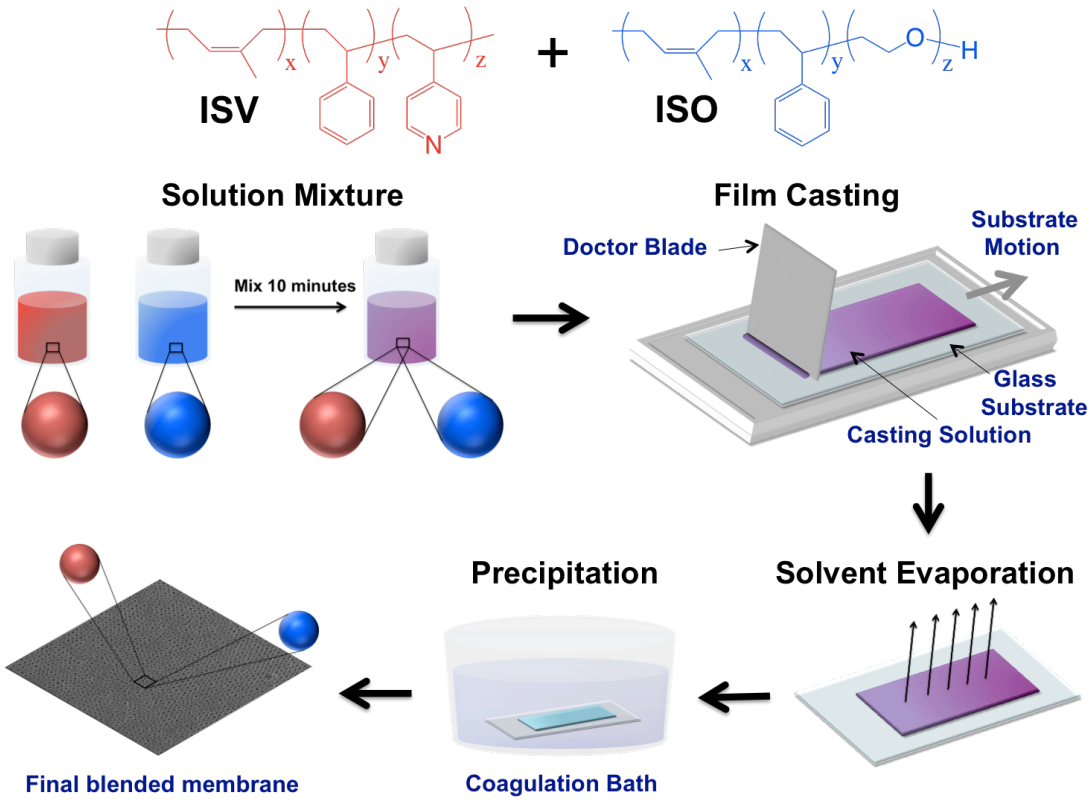

Figure 3.1. The chemical structures of ISV and ISO and a schematic depicting the procedure used for blending ISV and ISO triblock terpolymers to form a blended membrane. Individual casting solutions of ISV and ISO were prepared in a solvent system of DOX/THF/MeCN (~67/28/5 wt%) and stirred overnight. The solutions were then mixed together for 10 minutes to form the blended casting solutions. Solutions were then casted into a polymer film by using a doctor blade set at a predetermined gate height. The solvents were then allowed to partially evaporate for 120 seconds, driving the block copolymer self-assembly process. Finally, this film was plunged into a coagulation bath to obtain the blended SNIPS membranes.

3.3.2 Membrane Fabrication and Characterization

Integral asymmetric mesporous membranes were fabricated by blending two triblock terpolymers during the SNIPS process as described previously.[28] A schematic depicting the blending process employed is shown in Figure 3.1.

A ternary solvent mixture of 1,4-dioxane (DOX), tetrahydrofuran (THF), and acetonitrile (MeCN) was used as the solvent system for both ISV and ISO triblock

terpolymers. The casting solutions were prepared by separately dissolving 11% ISV and 18% ISO in a solvent system consisting of DOX/THF/MeCN (~67/28/5 wt%) at 300 rpm overnight. The individual casting solutions were then mixed and stirred together at 300 rpm for 10 minutes to form blended casting solutions with ISV + ISO weight ratios of 9:1, 7:3, and 5:5. A pure ISV membrane was prepared as a reference for comparison.

The dope solution was pipetted onto a glass substrate and a thin film was casted using an automated blade-casting machine permitting substrate motion with the gate height set between 203 μm and 229 μm. The solvent was allowed to partially evaporate from the thin film for 120 seconds before precipitating it into a coagulation bath of 18.2 MΩ deionized water. The solvent evaporation step is critical to drive the self-assembly of the triblock terpolymers and is responsible for the thin selective mesoporous skin layer atop the macroporous substructure of the resultant asymmetric membrane. The final membranes were separated from the glass substrate and stored in deionized water until tested.

Scanning electron microscopy (SEM) micrographs were obtained using a Tescan Mira3 field emission scanning electron microscope (FE-SEM) at an acceleration voltage of 5 kV and a working distance of 3-5 mm. The membrane samples were dried and sputter coated with gold-palladium using a Denton Vacuum Desk II for 8 seconds prior to imaging.

The micrographs obtained were analyzed using Mathematica and Image J softwares to determine pore size, pore density and porosity of the membrane top surfaces. The average values were calculated from analysis of two SEM images for

each sample.

3.3.3 Membrane Performance Tests

pH-responsive Permeability Tests

Membranes with an active area of 4.1 cm^2 were punched out and pH-responsive permeability tests were performed using a dead-end stirred cell (Amicon 8010, Millipore, Co.) connected to a nitrogen gas source. To prevent damage of the membrane from the stirred cell, the membranes were placed on a 0.2 μm nylon support (Sterlitech) during testing. pH buffers of sodium acetate and acetic acid were used for pH values in the range of 3-6, while pH buffers of imidazole and hydrochloric acid were used for the 7-8 pH range. The pH values of the buffer solutions were measured with a pH probe prior to permeability tests. Three measurements were conducted for each sample at varying trans membrane pressures of 1, 2, and 3 psi and the average values were reported.

Protein Adsorption Tests

Membranes with an area of about 2.01 cm^2 were used to determine protein adsorption. Solutions with a concentration of 1 g/L of bovine serum albumin (BSA) and γ-globulin (IgG) in a phosphate buffered saline (PBS) solution (pH ~7.5) were separately prepared. The membranes were soaked in 3 mL of the protein solution (soak solution) and continuously shaken for 24 hours to allow protein adsorption. Membranes were then immersed in a PBS solution containing no protein (wash solution) and shaken for 10 minutes to remove reversibly attached protein. The

concentration of these two solutions was determined using a Bradford Assay,[30] by observing the absorbance at a wavelength of 595 nm with UV-visible spectroscopy and comparing the values to a standard calibration. The protein adsorbed onto the membrane was determined as follows:

$$\text{Adsorbed Protein} = \frac{m_0 - (m_s + m_w)}{A} \tag{3.3.1}$$

m_0 is the mass of protein in soak solution prior to the test, m_s is the mass of protein in soak solution after the test, m_w is the mass of reversibly attached protein in wash solution, and A is the membrane area. For each protein, three repeats were performed per sample and the average value was reported in μg/cm^2.

3.4 Results and Discussion

3.4.1 Membrane Characterization

The top surface, bottom surface, and cross-section of the parent ISV and blended ISV:ISO membranes are shown in the first, second, and third rows of Figure 3.2. A magnified view of a selected region on the bottom surface is shown in the inset of the second row. The SEM micrographs of pure ISV, 9:1 blend, and 7:3 blend membranes depict relatively ordered pores on the top structure in a 2D square lattice pore arrangement, as confirmed by two-dimensional fast Fourier Transform (FFT) analysis (see Figure B.2). The top surface SEM images (Figure 3.2 first row) depict increasing disorder with the growing amount of ISO added into the blend. This observation is consistent with the fact that the pure ISO membrane does not portray an ordered top surface under similar conditions used in this study (see Figure B.3). Except for the membrane fabricated from the 5:5 blend, all the membranes used in this study have relatively open bottom surfaces (Figure 3.2 second row and inset) and finger-like cross-sections (Figure 3.2 third row).

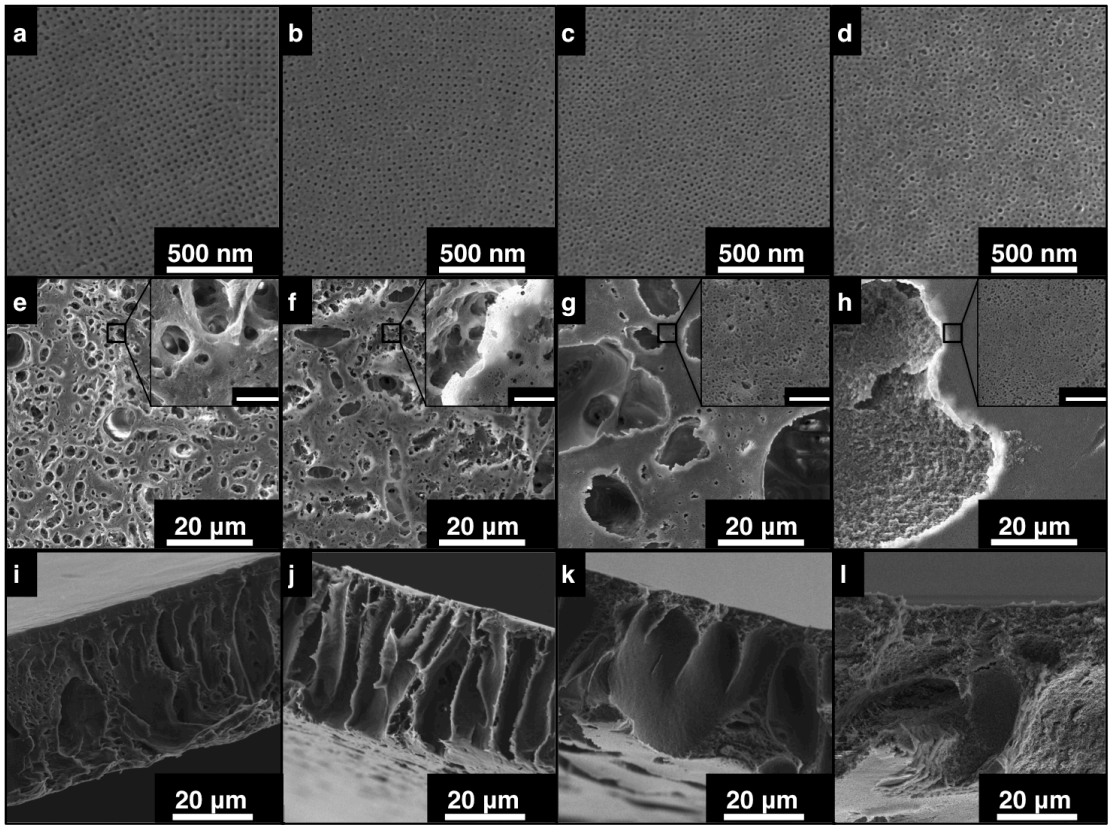

Figure 3.2. SEM micrographs of pure and blended SNIPS membranes. Top surfaces (first row), bottom surfaces and higher magnification images of selected regions (second row and insets, respectively), and cross-sectional images (third row) of asymmetric membranes fabricated using (a,e,i) ISV, (b,f,j) 9:1 ISV:ISO Blend, (c,g,k) 7:3 ISV:ISO Blend, and (d,h,l) 5:5 ISV:ISO Blend. Each polymer solution (11% ISV and 18% ISO) was prepared in a solvent system of DOX/THF/MeCN (~67/28/5 wt%). For the blended membrane preparation, solutions of individual polymer components were mixed for 10 minutes at 300 rpm before casting. The polymer films were evaporated for 120 seconds prior to plunging in the coagulation bath. The scale bars for inset images in the second row are 2 µm.

The top surface SEM images of the membranes were analyzed using Mathematica and Image J software to determine the average values of pore size, pore density, and porosity with results listed in Table 3.2. All the membranes analyzed show nearly similar values of pore size and the same order of magnitude for pore density. No clear trend in surface porosity was observed from this analysis.

Table 3.2. Average values for pore size, pore density, and porosity of top surfaces of pure and blended membranes. Pore size and pore density were calculated using Mathematica and surface porosity was calculated using Image J.

System	Average Pore Size (nm)	Average Pore Density (pores m^{-2})	Average Porosity (%)
ISV	21.0 ± 0.1	5.1×10^{14}	18
9:1 Blend	19.1 ± 0.8	7.3×10^{14}	10
7:3 Blend	21.6 ± 0.4	7.4×10^{14}	15
5:5 Blend	23.8 ± 0.1	2.5×10^{14}	8

3.4.2 Membrane Performance Testing

The hydraulic permeability was tested of pure and blended membranes as a function of the feed solution's pH. A pressurized dead-end stirred cell was used with 10 mL of buffer feed solutions at varying pH values (Experimental section). For each data point, three values at pressure drops of 1, 2, and 3 psi were measured. The average values of permeability as a function of varying pH are reported in Figure 3.3.

In this work, the permeability of ~1800 LMH/bar at pH values of 5 and above for pure ISV is consistent with results for other ISV terpolymers studied before and is due to the collapsed structure of P4VP brushes lining the membrane pores.[16,28] At pH values lower than the pK_a of P4VP (4.6), the hydraulic permeability drastically drops. This is due to the protonation of P4VP brushes, which extend outward towards the center of the pore thereby reducing the effective pore size.[16,31,32] The flow of feed solution through the membrane pores is thus restricted and leads to a reduced average

permeability. For the 9:1 and 7:3 ISV:ISO blended membranes, this membrane pH-responsiveness is preserved. The pH-responsive flux measurements were reproduced for an independent set of pure and blended membranes (see Figure B.4). Results suggest that in the blends the ISV blocks remain at the pore surface thereby continuing to enable pH dependent responsiveness. Furthermore, the reduction in membrane permeability with decreasing feed pH, irrespective of blend composition, suggests that there are no major defects in these membranes.

As the ratio of ISO in the blend increases, an overall decrease in the permeability is observed. From the image analysis of the membrane top surface (Table 3.2), no clear trend in the top surface pore size or pore density as a function of varying blend ratio was observed. Hence, membrane top surfaces structure is not a good measure to rationalize the trend seen in the permeability profiles. This implies that the decrease in permeability is likely due to composition dependent structure variations in membrane substructure.

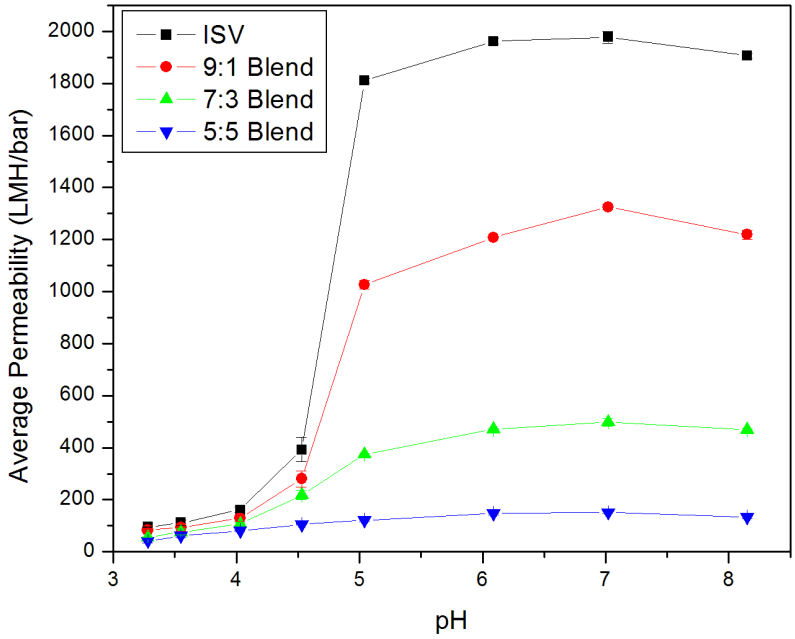

Figure 3.3. Average permeability of pure ISV and blended (9:1, 7:3, 5:5) ISV:ISO membranes as a function of varying pH values of feed solution. Indicated errors are standard deviations from three replicate measurements performed at 1, 2, and 3 psi transmembrane pressure drop.

3.4.3 Protein Adsorption Resistance Testing

The susceptibility of membranes that have P4VP lining the pore walls to protein fouling has been studied before.[19] Several studies aimed to reduce the protein adsorption of block copolymer membranes by leveraging the anti-fouling behavior of PEO due to its hydrophilicity.[15-27] In this study, the successful incorporation of the triblock terpolymer, ISO, blended into SNIPS membranes is tested through its characteristic property of reducing protein adsorption.

To measure the resistance to protein adsorption of pure and blended membranes, 3 mL of a 1 g/L solution containing one of two model proteins, bovine

serum albumin (BSA) and γ-globulin (IgG), were used to foul the membranes. For each membrane sample, three repeats were performed and the average value is reported in μg/cm^2. As seen in Figure 3.4. for both BSA and IgG, the amount of protein adsorbed decreased as the amount of ISO increased. Specifically, in the case of both proteins, about a threefold decrease in protein adsorption was observed between pure ISV and the 5:5 ISV:ISO blend. This can be rationalized by the addition of the hydrophilic PEO block in the blended membrane.[20,21] As more ISO is added, the hydrophilic character of the membrane surface increases and makes the membrane more resistant to protein adsorption. Through simple compositional control of the polymer dope used to fabricate these blended membranes, while maintaining pH responsiveness we are able to simultaneously demonstrate the ability to tune adsorption properties of the membranes pore surfaces. Thus, this facile blending approach combined with the SNIPS process is a powerful tool to introduce unique chemical functionalities of UF membranes.

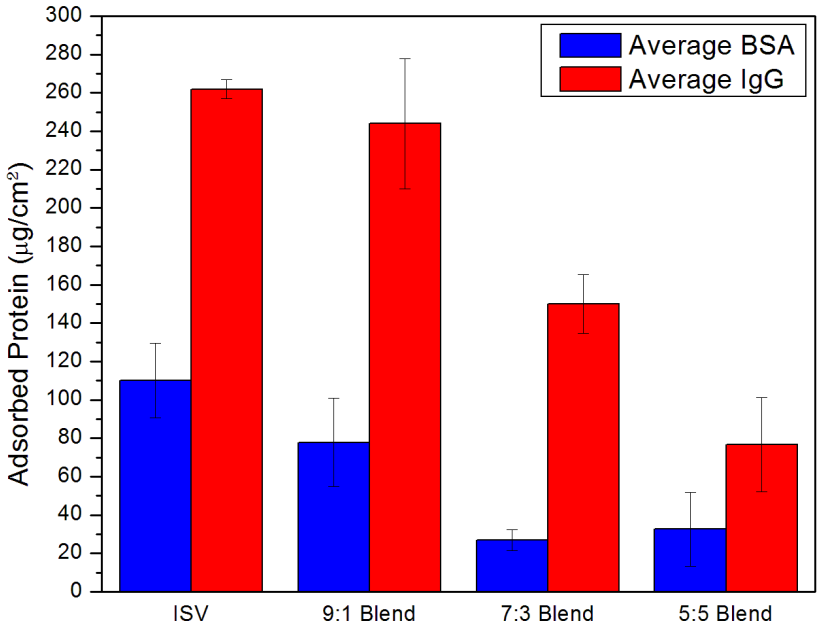

Figure 3.4. Comparison of BSA (bovine serum albumin) and IgG (γ-globulin) model proteins adsorbed on pure and blended membranes.

In this article, we applied the SNIPS process to two chemically distinct triblock terpolymers, ISV and ISO, in order to incorporate them into a single membrane. The fabricated blended asymmetric membranes exhibit unique chemical functionalities in the form of pH-responsiveness and anti-fouling characteristics intrinsic to their parent hydrophilic terpolymer blocks. Furthermore, the weight ratio of parent ISV and ISO in the blended polymer dope tailored the final properties of the resultant membranes. Therefore, this simple blending approach to the SNIPS process proves to be a promising way to "mix and match" chemical surface properties within the final membrane pores.

3.5 Conclusion

This study provided insights into the potentials and limitations of the blending approach. For example, the challenge of producing standalone ISO membranes with competitive final properties could be overcome through simple mixing of ISO into a terpolymer blend. The work further demonstrated that different concentrations of the parent block copolymers resulted in functional blended membranes. However, while the 5:5 ISV:ISO blend showed superior resistance to protein adsorption, it showed limited pH-responsive behavior and a relatively low overall permeability level.

The ability to fabricate asymmetric block copolymer membranes using SNIPS that exhibit ordered top surface pores, open substructures, high values of permselectivity and stimuli-responsive behavior has provided new directions for the search of advanced UF membranes. The ability of adding anti-fouling characteristics to these aforementioned properties through a facile "mix and match" approach improves the suitability of this approach for various applications including protein separation important e.g. for the biopharmaceuticals industry. In a wider context, the work poses interesting scientific questions regarding the mechanism, control, capabilities, and constraints of the SNIPS process utilizing the block copolymer "mixing and matching" approach. By gaining insights into these fundamental aspects, we might be able to further expand the property profile of this interesting class of porous materials.

Acknowledgements

P.N.V. would like to acknowledge the funding of this project by Contract No. HDTRA1-13-C0003 from the Defense Threat Reduction Agency (DTRA). This work utilized the facilities provided by the Cornell Center for Materials Research (CCMR) supported by NSF MRSEC program (DMR-1120296) and the Cornell Nanobiotechnology Center (NBTC). P.N.V. thanks Q. Zhang and F. Matsuoka from the Wiesner group for help in the block copolymer synthesis.

3.6 Appendix B

3.6.1 Membrane top surface analyses

For all SNIPS membranes investigated, top surface SEM images were utilized for pore size distribution and FFT analyses.

The pore size distribution was calculated using Image J software and a log-normal fit of the histograms were obtained using MATLAB. The histograms for the pore size distribution of the individual blended membranes and the corresponding log-normal fit curves are shown in Figure B.1 (a-d). A comparative analysis of all the log-normal fits obtained for the various blends is represented in Figure B.1 (e). As the amount of ISO in the blends increases, a corresponding wider spread of the pore size is observed.

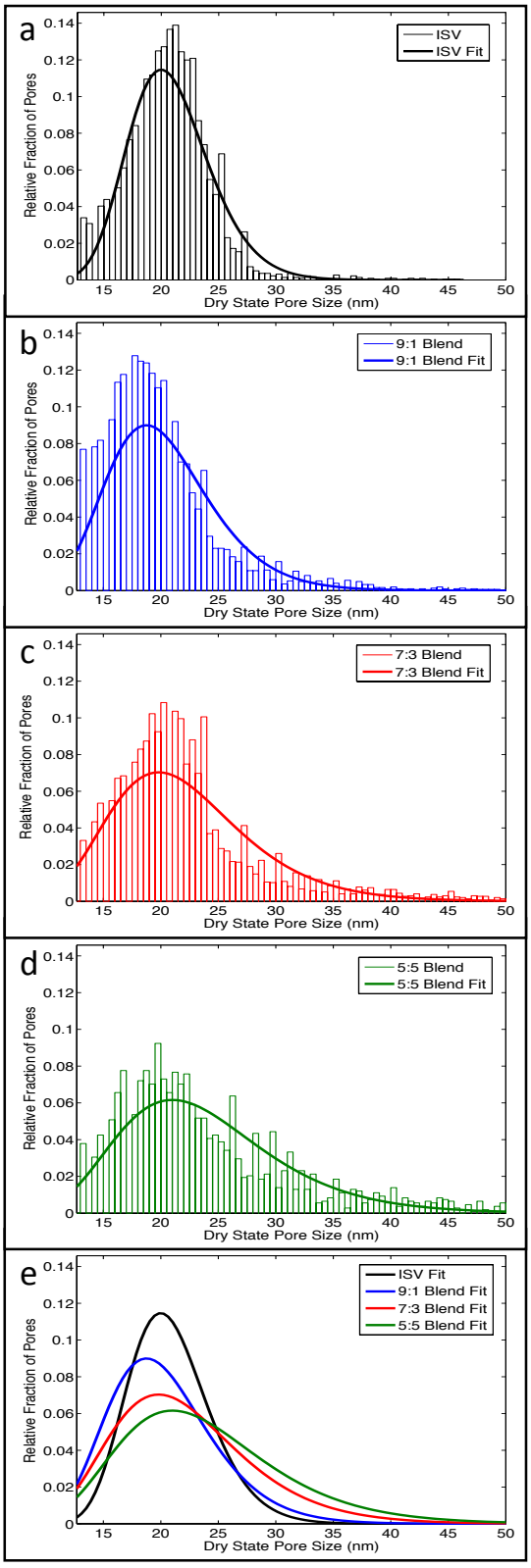

Figure B.1. Pore size distributions of parent (ISV) and blended membrane top surface layers (as indicated) obtained from SEM image analysis. The top surface SEM images were analyzed by Image J to calculate pore size distributions that were subsequently fit using a log-normal distribution.

The top surface SEM images of the membranes analyzed using Image J were also used to calculate two-dimensional Fast Fourier transforms (FFTs). Similar to the pure ISV membrane, FFTs of the 9:1 and 7:3 blended membranes were consistent with a 2D square lattice pore arrangement (see ticks in Figure B.2). Resulting pore-to-pore distances (*d*) for the membranes are indicated in the figure.

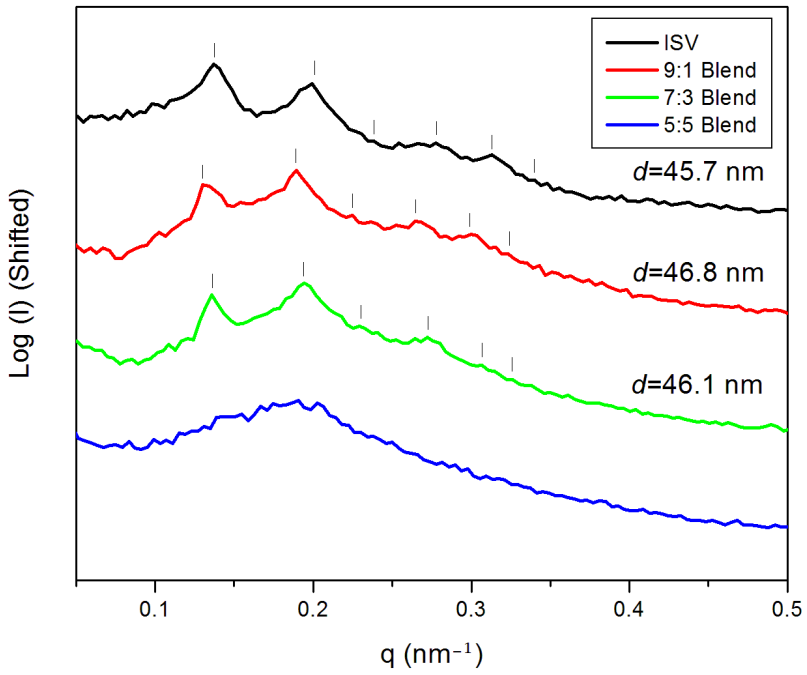

Figure B.2. The radially integrated FFT analysis of SEM images of the top surfaces of parent (ISV) and blended membranes investigated in this study, indexed with a 2D square lattice (see ticks) and corresponding pore-to-pore distances, *d*.

3.6.2 SEM micrographs of pure ISO membrane

SEM images of a pure SNIPS derived ISO membrane is shown in Figure B.3. The top surface SEM image suggests a lack of pore order. As shown in Figure 3.2 of the main text, an increase in the amount of ISO added to the blend led to more disorder in the

top surfaces as revealed by SEM imaging. This result is consistent with the disordered top surface observed here for the pure ISO membrane.

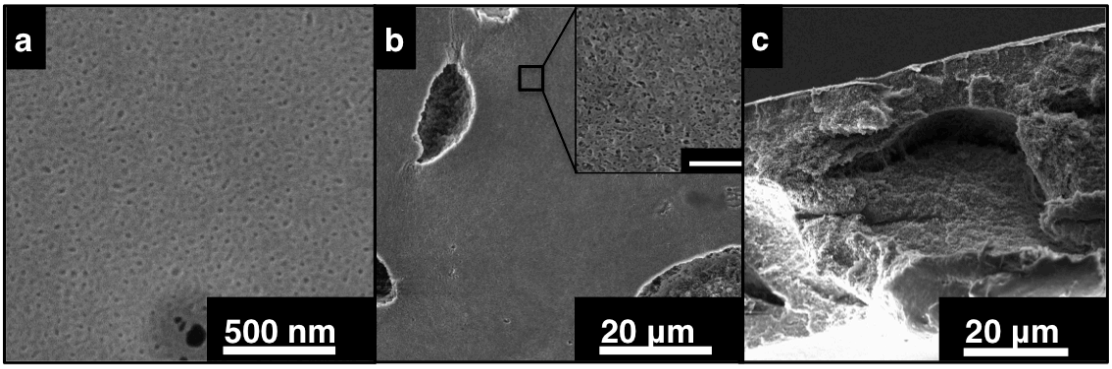

Figure B.3. SEM images of a pure ISO derived SNIPS membrane. (a) Top surface, (b) bottom, and (c) cross-section of a membrane derived from 18% ISO dissolved in a solvent system of DOX/THF/MeCN (~67/28/5 wt%) and evaporated for 80 sec prior to plunging into a DI water coagulation bath. The scale bar for the image in the inset in (b), which is a magnified view of a selected region of the bottom surface, is 2 µm.

3.6.3 Membrane Performance Testing

A separate set of parent ISV and blended membranes (9:1, 7:3, and 5:5 blends of ISV:ISO) were analyzed in terms of pH-dependent flux properties. For each feed solution, three replicate measurements were performed at 1, 2, and 3 psi trans-membrane pressure and an average value of permeability was calculated as shown in Figure B.4. The analysis yielded consistent results with the first set of membranes shown in Figure 3.3 of the main text.

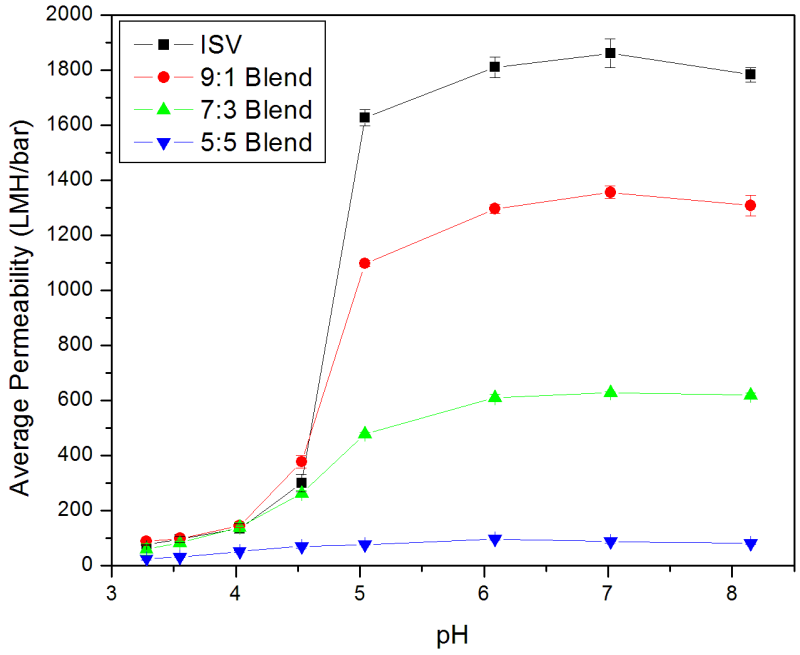

Figure B.4. pH-dependent permeability testing performed on a second set of parent ISV and blended ISV:ISO SNIPS derived membranes. Three replicate tests at 1, 2, and 3 psi pressure drops were performed for every feed buffer solution. Error bars indicate standard deviations obtained from these replicate measurements.

3.6.4 Contact Angle Testing

To determine the hydrophilicity of the membranes, water contact angle testing was performed using the sessile drop technique. A ramé-hart Model 500 Advanced Goniometer equipped with DROPimage Advanced software was employed for the analyses. Measurements were performed at randomly selected regions of the membrane samples with 10 µL deionised water droplets. For each sample, an average of three such readings at time t=0 was determined and reported in Figure B.5. No clear trend in the static contact angles was observed as a function of composition of the membranes.

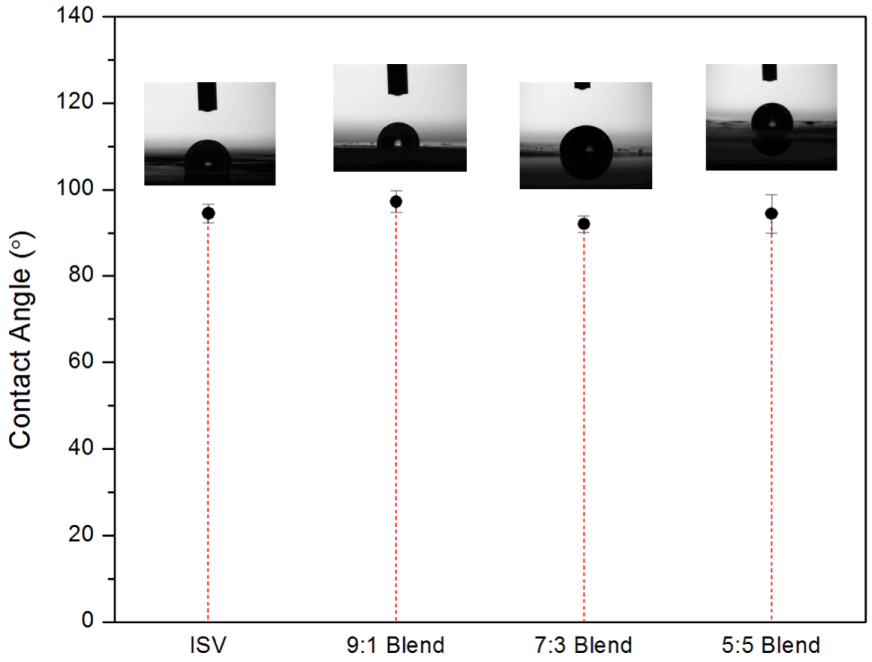

Figure B.5. Contact angle measurements performed on the parent (ISV) and ISV:ISO blended membranes. A 10 μL water droplet was used for each measurement and an average of the values measured at three randomly selected portions of the sample was reported.

A schematic depicting the top surface composition of the membranes is shown in Figure B.6. The majority of the membrane top surface is expected to be made up of either the hydrophobic matrix of poly(isoprene) and poly(styrene) or of the pore void. Only a very small portion of the top surface is expected be covered by the poly(4-vinyl-pyridine) or poly(ethylene oxide) blocks to form the pore walls depicted in the schematic as blue. Therefore, the influence of the hydrophilicity of this pore wall on the contact angle is expected to be small relative to everything else. This may explain why contact angle measurements were so insensitive to the change in the pore wall composition. In contrast, protein adsorption tests described in the main text (see Figure 3.4) were quite sensitive to the changing hydrophilicity of the pore walls as a

function of blend composition.

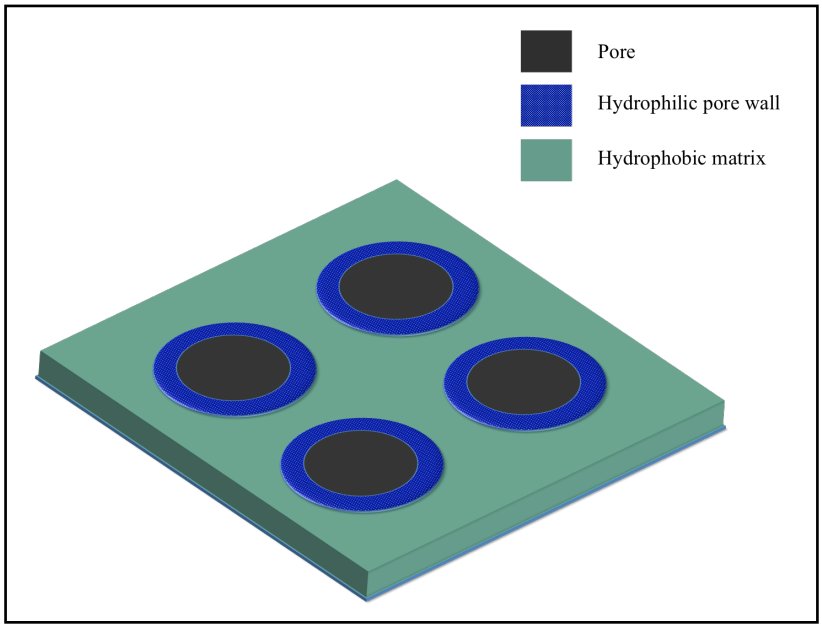

Figure B.6. A schematic representing the top surface of a SNIPS derived membrane. The pore walls made up of the hydrophilic component of the block copolymers have a much lower surface area as compared to the combined area of the hydrophobic matrix made of poly(isoprene) and poly(styrene) and the pore void.

3.7 References

1. Peinemann, K.V.; Abetz, V.; Simon, P. F. W. Asymmetric superstructure formed in a block copolymer via phase separation. *Nat. Mater.* **2007**, 6 (12), 992–996.
2. Dorin, R. M.; Marques, D. S.; Sai, H.; Vainio, U.; Phillip, W. A.; Peinemann, K.V.; Nunes, S. P.; Wiesner, U. Solution Small-Angle X-ray Scattering as a Screening and Predictive Tool in the Fabrication of Asymmetric Block Copolymer Membranes. *ACS Macro Lett.* **2012**, 1 (5), 614–617.
3. Pendergast, M. M.; Dorin, R. M.; Phillip, W. A.; Wiesner, U.; Hoek, E. M. Understanding the structure and performance of self-assembled triblock terpolymer membranes. *J. Membr. Sci.* **2013**, 444, 461–468.
4. Dorin, R. M.; Phillip, W. A.; Sai, H.; Werner, J.; Elimelech, M.; Wiesner, U. Designing block copolymer architectures for targeted membrane performance. *Polymer* **2014**, 55 (1), 347–353.
5. Rangou, S.; Buhr, K.; Filiz, V.; Clodt, J. I.; Lademann, B.; Hahn, J.; Jung, A.; Abetz, V. Self-organized isoporous membranes with tailored pore sizes. *J. Membr. Sci.* **2014**, 451, 266–275.
6. Gu, Y.; Wiesner, U. Tailoring pore size of graded mesoporous block copolymer membranes: moving from ultrafiltration toward nanofiltration. *Macromolecules* **2015**, 48 (17), 6153–6159.
7. Radjabian, M.; Abetz, V. Tailored pore sizes in integral asymmetric membranes formed by blends of block copolymers. *Adv. Mater.* **2014**, 27 (2), 352–355.

8. Zhang, Q.; Li, Y. M.; Gu, Y.; Dorin, R. M.; Wiesner, U. Tuning substructure and properties of supported asymmetric triblock terpolymer membranes. *Polymer* **2016**, 107, 398–405.
9. Nunes, S. P.; Sougrat, R.; Hooghan, B.; Anjum, D. H.; Behzad, A. R.; Zhao, L.; Pradeep, N.; Pinnau, I.; Vainio, U.; Peinemann, K.V. Ultraporous films with uniform nanochannels by block copolymer micelles assembly. *Macromolecules* **2010**, 43 (19), 8079–8085.
10. Nunes, S. P.; Karunakaran, M.; Pradeep, N.; Behzad, A. R.; Hooghan, B.; Sougrat, R.; He, H.; Peinemann, K.V. From micelle supramolecular assemblies in selective solvents to isoporous membranes. *Langmuir* **2011**, 27 (16), 10184–10190.
11. Clodt, J. I.; Rangou, S.; Schröder, A.; Buhr, K.; Hahn, J.; Jung, A.; Filiz, V.; Abetz, V. Carbohydrates as additives for the formation of isoporous PS-b-P4VP diblock copolymer membranes. *Macromol. Rapid Commun.* **2012**, 34 (2), 190–194.
12. Marques, D. S.; Dorin, R. M.; Wiesner, U.; Smilgies, D.-M.; Behzad, A. R.; Vainio, U.; Peinemann, K.-V.; Nunes, S. P. Time-resolved GISAXS and cryo-microscopy characterization of block copolymer membrane formation. *Polymer* **2014**, 55 (6), 1327–1332.
13. Radjabian, M.; Abetz, C.; Fischer, B.; Meyer, A.; Abetz, V. Influence of solvent on the Structure of an Amphiphilic Block Copolymer in Solution and in Formation of an Integral Asymmetric Membrane. *ACS Appl. Mater. Inter.* **2017**.

14. Jung, A.; Rangou, S.; Abetz, C.; Filiz, V.; Abetz, V. Structure Formation of Integral Asymmetric Composite Membranes of Polystyrene-block-Poly (2-vinylpyridine) on a Nonwoven. *Macromol. Mater. Eng.* **2012**, 297 (8), 790–798.
15. Shevate, R.; Karunakaran, M.; Kumar, M.; Peinemann, K.-V. Polyanionic pH-responsive polystyrene-b-poly (4-vinyl pyridine-N-oxide) isoporous membranes. *J. Membr. Sci.* **2016**, 501, 161–168.
16. Phillip, W. A.; Dorin, R. M.; Werner, J.; Hoek, E. M. V.; Wiesner, U.; Elimelech, M. Tuning structure and properties of graded triblock terpolymer-based mesoporous and hybrid films. *Nano Lett.* **2011**, 11 (7), 2892–2900.
17. Mulvenna, R. A.; Weidman, J. L.; Jing, B.; Pople, J. A.; Zhu, Y.; Boudouris, B. W.; Phillip, W. A. Tunable nanoporous membranes with chemically-tailored pore walls from triblock polymer templates. *J. Membr. Sci.* **2014**, 470, 246–256.
18. Zhang, Q.; Gu, Y.; Li, Y. M.; Beaucage, P. A.; Kao, T.; Wiesner, U. Dynamically responsive multifunctional asymmetric triblock terpolymer membranes with intrinsic binding sites for covalent molecule attachment. *Chem. Mater.* **2016**, 28 (11), 3870–3876.
19. Hahn, J.; Clodt, J. I.; Filiz, V.; Abetz, V. Protein separation performance of self-assembled block copolymer membranes. *RSC Adv.* **2014**, 4 (20), 10252.
20. Rana, D.; Matsuura, T. Surface modifications for antifouling membranes. *Chem. Rev.* **2010**, 110 (4), 2448–2471.

21. Park, J.; Acar, M.; Akthakul, A.; Kuhlman, W.; Mayes, A. Polysulfone-graft-poly (ethylene glycol) graft copolymers for surface modification of polysulfone membranes. *Biomaterials* **2006**, 27 (6), 856–865.
22. Dong, B.; Jiang, H.; Manolache, S.; Wong, A. C. L.; Denes, F. S. Plasma-mediated grafting of poly (ethylene glycol) on polyamide and polyester surfaces and evaluation of antifouling ability of modified substrates. *Langmuir* **2007**, 23 (13), 7306–7313.
23. Asatekin, A.; Kang, S.; Elimelech, M.; Mayes, A. M. Anti-fouling ultrafiltration membranes containing polyacrylonitrile-graft-poly (ethylene oxide) comb copolymer additives. *J. Membr. Sci.* **2007**, 298 (1-2), 136–146.
24. Wang, Y. Q.; Wang, T.; Su, Y. L.; Peng, F. B.; Wu, H.; Jiang, Z. Y. Remarkable reduction of irreversible fouling and improvement of the permeation properties of poly (ether sulfone) ultrafiltration membranes by blending with pluronic F127. *Langmuir* **2005**, 21 (25), 11856–11862.
25. Hahn, J.; Filiz, V.; Rangou, S.; Clodt, J.; Jung, A.; Buhr, K.; Abetz, C.; Abetz, V. Structure formation of integral-asymmetric membranes of polystyrene-block-Poly (ethylene oxide). *J. Polym. Sci., Part B: Polym. Phys.* **2012**, 51 (4), 281–290.
26. Karunakaran, M.; Nunes, S. P.; Qiu, X.; Yu, H.; Peinemann, K.V. Isoporous PS-b-PEO ultrafiltration membranes via self-assembly and water-induced phase separation. *J. Membr. Sci.* **2014**, 453, 471–477.
27. Jung, A.; Filiz, V.; Rangou, S.; Buhr, K.; Merten, P.; Hahn, J.; Clodt, J.; Abetz, C.; Abetz, V. Formation of integral asymmetric membranes of AB diblock and

ABC triblock copolymers by phase inversion. *Macromol. Rapid Commun.* **2013**, 34 (7), 610–615.

28. Li, Y. M.; Srinivasan, D.; Vaidya, P.; Gu, Y.; Wiesner, U. Asymmetric Membranes from Two Chemically Distinct Triblock Terpolymers Blended during Standard Membrane Fabrication. *Macromol. Rapid Commun.* **2016**, 37 (20), 1689–1693.
29. Robbins, S. W.; Sai, H.; Disalvo, F. J.; Gruner, S. M.; Wiesner, U. Monolithic Gyroidal Mesoporous Mixed Titanium–Niobium Nitrides. *ACS Nano* **2014**, 8 (8), 8217–8223.
30. Bradford, M. M. A rapid and sensitive method for the quantitation of microgram quantities of protein utilizing the principle of protein-dye binding. *Anal. Biochem.* **1976**, 72 (1-2), 248–254.
31. Clodt, J. I.; Filiz, V.; Rangou, S.; Buhr, K.; Abetz, C.; Höche, D.; Hahn, J.; Jung, A.; Abetz, V. Double Stimuli-Responsive Isoporous Membranes via Post-Modification of pH-Sensitive Self-Assembled Diblock Copolymer Membranes. *Adv. Funct. Mater.* **2012**, 23 (6), 731–738.
32. Nunes, S. P.; Behzad, A. R.; Hooghan, B.; Sougrat, R.; Karunakaran, M.; Pradeep, N.; Vainio, U.; Peinemann, K.V. Switchable pH-responsive polymeric membranes prepared via block copolymer micelle assembly. *ACS Nano* **2011**, 5 (5), 3516–3522.

CHAPTER 4

OUTLOOK

Block copolymer membranes prepared using SNIPS process hold tremendous promise for use in ultrafiltration, protein separation and biopharmaceutical applications. In recent years, a lot of work has been performed to expand the library of block copolymers submitted to SNIPS, including triblock terpolymers like poly(isoprene-*b*-styrene-*b*-*N*,*N*-dimethylacrylamide)[1] and poly(styrene-*b*-4-vinylpyridine-*b*-propylene sulfide).[2] Furthermore, extensive work is being carried out to determine the underlying mechanisms involved in SNIPS to deduce concrete formulation-structure-property relationships. For example, one study used solution small-angle X-ray scattering (SAXS) to quickly screen solutions suitable for desired final membrane structure.[3] Another study aimed at reducing time required to get optimized systems for SNIPS membranes using segregation strength trend lines.[4]

However, extending SNIPS process to a new library of block copolymers still involves tedious optimization steps using trial and error, often requiring control over as many as 20 parameters. In this thesis, we successfully demonstrated the use of a powerful "mix and match" technique to overcome this problem. In principle, we can mix a desired chemical functionality into the membrane pore surface without the need to use complex post-functionalization methods previously employed.[5]

Much work still needs to be done before we can fully unveil the potential of this blending approach. For example, there are several pending questions regarding the kinetics and mechanisms of the blending process. Studies exploring the mixing

behavior of the polymer micelles as a function of mixing time (as depicted in Figure 4.1) might provide useful insights. There is a possibility to explore a threshold time required for mixing that might directly impact the final distribution of chemical groups within the membranes.

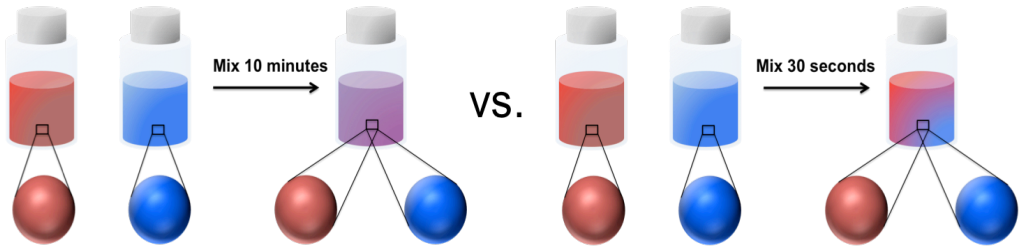

Figure 4.1. A schematic depicting a temporal study of the blending mechanism in the dope solution prior to SNIPS membrane fabrication.

Furthermore, this method might be extended to mixing in more than two functionalities at a time in the polymer dope solution (as shown in Figure 4.2). By mixing in multiple functionalities in defined ratios, we might be able to provide more ways to control the final membrane surface properties. It would also be interesting to explore properties of block copolymers of different number of blocks blended together. For example, a diblock copolymer and a triblock terpolymer with the same or different chemical functionality might be blended in dope solution prior to SNIPS.

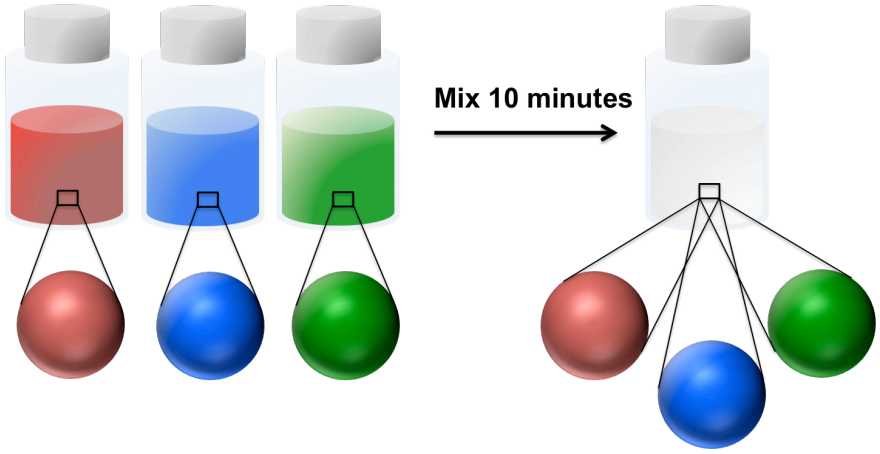

Figure 4.2. A schematic depicting blending of three distinct block copolymers in the dope solution prior to SNIPS membrane fabrication.

The blending approach to the SNIPS process provides yet another rich platform for exploring interesting properties of these membranes, the mechanism of their formation, and promising industrial applications. The versatility of SNIPS process and the potential of the blending approach bring us another step closer to making designer cutting-edge membranes for targeted applications.

References

1. Mulvenna, R. A.; Weidman, J. L.; Jing, B.; Pople, J. A.; Zhu, Y.; Boudouris, B. W.; Phillip, W. A. Tunable nanoporous membranes with chemically-tailored pore walls from triblock polymer templates. *J. Membr. Sci.* **2014**, 470, 246–256.
2. Zhang, Q.; Gu, Y.; Li, Y. M.; Beaucage, P. A.; Kao, T.; Wiesner, U. Dynamically responsive multifunctional asymmetric triblock terpolymer membranes with intrinsic binding sites for covalent molecule attachment. *Chem. Mater.* **2016**, 28 (11), 3870–3876.
3. Dorin, R. M.; Marques, D. S.; Sai, H.; Vainio, U.; Phillip, W. A.; Peinemann, K.V.; Nunes, S. P.; Wiesner, U. Solution small-angle X-ray scattering as a screening and predictive tool in the fabrication of asymmetric block copolymer membranes. *ACS Macro Lett.* **2012**, 1 (5), 614–617.
4. Sutisna, B.; Polymeropoulos, G.; Musteata, V.; Peinemann, K.V.; Avgeropoulos, A.; Smilgies, D.M.; Hadjichristidis, N.; Nunes, S. P. Design of block copolymer membranes using segregation strength trend lines. *Mol. Syst. Des. Eng.* **2016**, 1 (3), 278–289.
5. Clodt, J. I.; Filiz, V.; Rangou, S.; Buhr, K.; Abetz, C.; Höche, D.; Hahn, J.; Jung, A.; Abetz, V. Double Stimuli-Responsive Isoporous Membranes via Post-Modification of pH-Sensitive Self-Assembled Diblock Copolymer Membranes. *Adv. Funct. Mater.* **2012**, 23 (6), 731–738.